Cell-free reconstitution of vacuole membrane fragmentation reveals regulation of vacuole size and number by TORC1

Lydie Michaillat, Tonie Luise Baars, and Andreas Mayer
Département de Biochimie, Université de Lausanne, 1066 Epalinges, Switzerland

ABSTRACT **Size and copy number of organelles are influenced by an equilibrium of membrane fusion and fission. We studied this equilibrium on vacuoles—the lysosomes of yeast. Vacuole fusion can readily be reconstituted and quantified in vitro, but it had not been possible to study fission of the organelle in a similar way. Here we present a cell-free system that reconstitutes fragmentation of purified yeast vacuoles (lysosomes) into smaller vesicles. Fragmentation in vitro reproduces physiological aspects. It requires the dynamin-like GTPase Vps1p, V-ATPase pump activity, cytosolic proteins, and ATP and GTP hydrolysis. We used the in vitro system to show that the vacuole-associated TOR complex 1 (TORC1) stimulates vacuole fragmentation but not the opposing reaction of vacuole fusion. Under nutrient restriction, TORC1 is inactivated, and the continuing fusion activity then dominates the fusion/fission equilibrium, decreasing the copy number and increasing the volume of the vacuolar compartment. This result can explain why nutrient restriction not only induces autophagy and a massive buildup of vacuolar/lysosomal hydrolases, but also leads to a concomitant increase in volume of the vacuolar compartment by coalescence of the organelles into a single large compartment.**

Monitoring Editor
Akihiko Nakano
RIKEN

Received: Aug 18, 2011
Revised: Dec 8, 2011
Accepted: Jan 4, 2012

INTRODUCTION

Numerous organelles fragment into smaller vesicles during cell division, vesicular traffic, or in response to changes in environmental conditions, changing the size, copy number, and morphology of these compartments. Examples include mitochondria (Yoon and McNiven, 2001; Shaw and Nunnari, 2002; Chan, 2006), plastids (Osteryoung and McAndrew, 2001), peroxisomes (Yan *et al.*, 2005; Schrader and Fahimi, 2006), endosomes (van der Goot and Gruenberg, 2006), the nuclear envelope (Newport and Forbes, 1987; Prunuske and Ullman, 2006), Golgi (Corda *et al.*, 2002; Shorter and Warren, 2002; Colanzi *et al.*, 2003; Rabouille and Jokitalo, 2003), lysosomes (Storrie and Desjardins, 1996), and vacuoles (Weisman, 2003). Whereas membrane fission of coated vesicles has been studied in considerable detail (Conner and Schmid, 2003; Mancias and Goldberg, 2005; McMahon and Gallop, 2005; Antonny, 2006), organelle fragmentation is less well understood. Genetic and biochemical approaches have identified a number of proteins and lipids involved in such reactions, but it is unclear how they cooperate to split organelles into smaller vesicles. Few organelle fragmentation reactions have been reconstituted in vitro: disassembly of the Golgi in mammalian cell extracts (Misteli and Warren, 1994; Rabouille *et al.*, 1995; Shorter and Warren, 1999) or in semi-intact cells (Acharya *et al.*, 1998; Kano *et al.*, 2000); the fission of endosomal/lysosomal hybrid organelles (Luzio *et al.*, 2003); and nuclear fragmentation (Newport and Forbes, 1987; Higa *et al.*, 2006) in *Xenopus* egg extracts. The cell-free reconstitution of these organelle fragmentation reactions has considerably supported the study of their mechanism.

Yeast vacuoles are relatively large (≤5 μm), so that their shape, size, and number during fragmentation are clearly visible in the light microscope. Size and copy number of yeast vacuoles change depending on the cell cycle stage and on environmental conditions (Weisman, 2003). Hypertonic shock induces rapid fragmentation of vacuoles into multiple small vesicles, whereas hypotonic treatment has the opposite effect. Nutrient restriction leads to a strong induction of vacuolar

This article was published online ahead of print in MBoC in Press (http://www.molbiolcell.org/cgi/doi/10.1091/mbc.E11-08-0703) on January 11, 2012.

Address correspondence to: Andreas Mayer (Andreas.Mayer@unil.ch).

Abbreviations used: GDI, GDP dissociation inhibitor; PI-3,5-P2, phosphatidylinositol-3,5-bisphosphate.

hydrolases and to a coalescence of all vacuoles of a cell into a single organelle, which provides increased volume (Baba *et al.*, 1994). Vacuole coalescence and fragmentation depend on the equilibrium of the activities of the vacuolar fusion and fission machineries, which thus determine vacuole morphology (Baars *et al.*, 2007). To study this equilibrium and the factors influencing it, it is desirable to be able to study fusion and fission separately.

For the study of vacuole fusion a powerful in vitro system has been established that makes it possible to measure this reaction with purified organelles in the test tube (Conradt *et al.*, 1994). The assay is based a mixture of two separately prepared vacuole populations—one containing an enzymatically inactive pro–alkaline phosphatase and the other one the necessary maturation enzyme (Haas *et al.*, 1994). Fusion will produce mature and active alkaline phosphatase, which serves as a tracer for fusion. This system has made it possible to identify many proteins and lipids implicated in vacuole fusion and to characterize multiple reaction intermediates (Ostrowicz *et al.*, 2008; Wickner, 2010). It has revealed that vacuole fusion shares many fundamental characteristics with other fusion reactions in cells, such as the requirement for soluble *N*-ethylmaleimide–sensitive factor attachment protein receptors, Rab-GTPases, Rab-effector proteins (homotypic fusion and vacuole protein sorting complex), and their control factors.

An in vitro system to study vacuole fission had not been available. However, because vacuoles fragment during the cell cycle or in hypertonic media, optical screening of mutants could identify mutants that show enlarged vacuoles and are defective in the salt-inducible fragmentation of vacuoles (Weisman, 2003; Efe *et al.*, 2005; LaGrassa and Ungermann, 2005). Crucial factors for vacuole fragmentation, such as the phosphatidylinositol-3-phosphate-5-kinase Fab1 and its effectors and regulators Vac7p, Vac14p, Fig4p, and Atg18p (Cooke *et al.*, 1998; Gary *et al.*, 1998, 2002; Bonangelino *et al.*, 2002; Dove *et al.*, 2002, 2004; Duex *et al.*, 2006a, 2006b; Efe *et al.*, 2007) are conserved between different eukaryotes, acting also on endosomal/lysosomal compartments in plants and mammals. In addition, the class C core vacuole/endosome tethering complex subunit Vps3p is required for fragmentation, and the casein kinase Yck3p is necessary to maintain the fragmented state under hypertonic conditions (LaGrassa and Ungermann, 2005; Peplowska *et al.*, 2007). Vacuole fragmentation also requires a dynamin-related GTPase, Vps1p (Peters *et al.*, 2004). This indicates a potential mechanistic similarity of vacuole fragmentation to the fragmentation of other organelles, in which dynamin-related GTPases have been implicated as well. Examples include mitochondria, peroxisomes, and chloroplasts (Bleazard *et al.*, 1999; Hoepfner *et al.*, 2001; Gao *et al.*, 2003; Li and Gould, 2003; Okamoto and Shaw, 2005; Kuravi *et al.*, 2006).

Here we report the cell-free reconstitution of the fragmentation of purified *Saccharomyces cerevisiae* vacuoles. We validated the authenticity of the cell-free reaction by studying the effects of mutations that generate defects of vacuole fragmentation in vivo. We demonstrate the utility of the in vitro approach by using it to identify a regulation of vacuole fragmentation by TOR kinase, confirm its relevance in vivo, and explore its role for regulating vacuole size and number.

RESULTS

Vacuolar membrane fission can be induced on isolated vacuoles

In living cells, vacuoles fragment during the cell cycle or in response to hypertonic shock (Weisman *et al.*, 1987; Catlett and Weisman, 2000). We attempted to reproduce vacuole fragmentation in a test tube with purified vacuoles. We incubated the organelles with ATP as an energy source and a cytosolic extract as a source of soluble proteins. After 1 h of incubation at 27°C, the membranes were stained with the lipophilic dye BODIPY FL-DHPE, and vacuolar morphology was visualized by confocal fluorescence microscopy. During the 60 min after the start of an in vitro fragmentation reaction, ≤90% of the large vacuoles that had been visible at the beginning fragmented into smaller vesicles (Figure 1, A and B) that often remained clustered together. We analyzed the size of the small fragmentation products by electron microscopy (Figure 1C). Fragmentation reactions incubated in the absence of ATP contained many intact vacuoles ($d = 2.1 \pm 0.6$ μm), visible as large circular structures with an electron-translucent, white lumen. After incubation with ATP, these large structures were absent, and numerous small vesicles ($d = 0.45 \pm 0.27$ μm) appeared. For routine analyses, vacuole fragmentation was analyzed by fluorescence microscopy. The organelles were quantified on confocal images taken from seven to 10 random fields and grouped into three classes according to their diameter: small ($d \leq 0.6$ μm), medium ($0.6 < d < 1.5$ μm), and large ($d \geq 1.5$ μm). Because clusters of the small vesicles are hard to resolve in the light microscope, their number could not be reliably determined by direct counting. Because their average diameter was known from electron microscopy, however, their number could be deduced from the surface they occupy in the image. Therefore we used this approach to assay the number of small vesicles. Electron microscopy (Figure 1C) showed that large vacuoles had an average surface of 12.5 μm^2 and the small vesicles of 0.64 μm^2. This suggests that a large vacuole could at most produce ~20 vacuolar fragments. In reasonable agreement with this, analysis of a fragmentation reaction (Figure 1B) from fluorescence micrographs according to the described procedure suggests that a large vacuole gave rise to ~17 fragments during the reaction. To facilitate comparisons, we defined a fragmentation index representing the degree of fragmentation. The proportion (R) of large vacuoles in the total vesicle pool of small (N_s), medium (N_m), and large (N_l) vacuoles is $R = N_l/(N_s + N_m + N_l)$. For the fragmentation index (FI) this proportion of large vacuoles is related to that in a positive control (R_{pos}), which is set to 100%: $FI = R_{pos}/R \times 100$ (%).

In vitro fragmentation activity increased with salt concentration, with optimal values obtained between 100 and 150 mM KAc (Figure 2A). Higher salt concentrations inhibited fragmentation. Activity was influenced by the type of salt. NaCl and KCl did not induce fragmentation, but NaAc supported fragmentation as well as KAc (Figure 2B). Sorbitol, used as a control for a nonionic but osmotically active substance, did not support fragmentation either. We decided to use KAc because K^+ ions are the predominant intracellular cation species. The salt dependence of vacuole fragmentation could have different reasons: Fragmentation into small vesicles increases the surface-to-volume ratio of the membranes, requiring extrusion of water. Exogenously added KAc might osmotically extract water and thus allow the vesicles to adjust their volume to the decreasing radius. Yet this cannot be the only factor because we could not replace KAc by sorbitol and because KAc concentrations >150 mM decreased fragmentation activity. It was also insufficient to provide just a certain ionic strength because the chloride salts could not substitute for the acetate salts. Thus a specific ionic milieu is required.

Vacuole fragmentation depends on the incubation temperature and on time. On ice, virtually no fragmentation was observed, whereas the efficiency of the reaction was maximal at 27°C (Figure 2C). Higher temperatures decreased apparent fragmentation. They even produced a fraction of vacuoles that were bigger than at the onset of the incubation (data not shown), suggesting that some

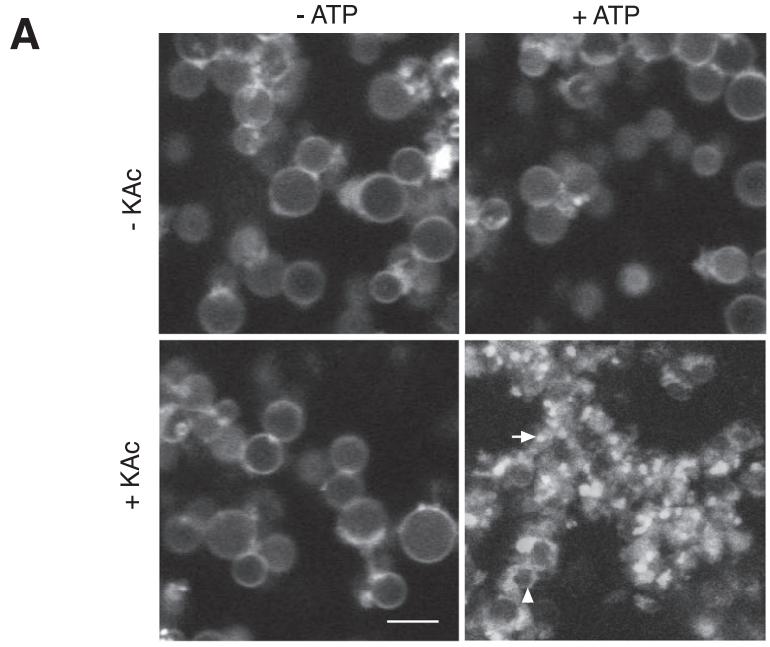

B

	N_s	N_m	N_l	N_t=N_s+N_m+N_l	R = N_l/N_t	FI = R_{pos}/R*100 (%)	
- KAc, - ATP	951	162	121	1234	0.098	2.7	
- KAc, +ATP	1111	110	53	1274	0.042	6.7	
+ KAc, - ATP	1416	200	117	1733	0.067	4.0	*
+ KAc, +ATP	2816	111	8	2935	(R_{pos})=0.0027	$1.0*10^2$	*

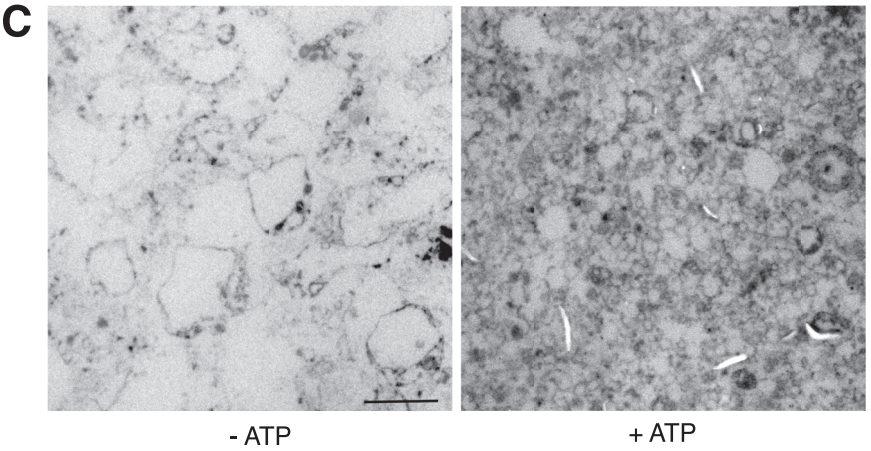

FIGURE 1: Vacuole fragmentation in vivo and in vitro. (A) Vacuoles were isolated from BJ3505 cells and subjected to in vitro fragmentation reactions. The membranes were stained with BODIPY-FL DHPE, fixed in cavity slides with 0.2% LMP-agarose, and visualized by confocal fluorescence microscopy. Examples for small (arrow) and medium-sized (arrowhead) vesicles are indicated. (B) Values for the numbers of vesicles of different diameter d: small (N_s; d ≤ 0.6 μm), medium (N_m; 0.6 <d < 1.5 μm), and large (N_l; d ≥ 1.5 μm). Vesicles were quantified and FI calculated as described in *Materials and Methods*. Of 121 large vacuoles, 113 were consumed during the reaction. The small-vesicle fraction increased from 951 to 2816, indicating a gain of 1865 small vesicles. This suggests that one large vacuole produced on average 1865/113 = 17 small vesicles. (C) Vacuoles were incubated in an in vitro fragmentation reaction in the presence or absence of ATP, fixed with glutaraldehyde, and analyzed by electron microscopy. Bars, 2 μm.

vacuoles might have fused. To test whether competing fusion activity might distort our results on fragmentation, time-course experiments were performed in the absence or presence of GDP dissociation inhibitor (GDI), a protein inhibiting fusion by inactivating the vacuolar Rab-GTPase Ypt7p (Figure 2D; Haas *et al.*, 1995). Vacuole fragmentation was determined 0, 20, 40, 60, and 90 min after starting a reaction (Figure 2E). After 60 min, most vacuoles had been converted into small vesicles, showing that in this phase of the incubation, fragmentation activity prevails. The time courses in the absence and presence of GDI overlapped up to the 60-min time point, indicating that the apparent fragmentation activity is not significantly diminished by fusion in this reaction phase. Later, vacuoles reappeared that were larger than the starting material, suggesting that fusion activity dominates the reaction after prolonged incubation times. This fusion activity can be demonstrated by an enzymatic fusion assay (see discussion and Figure 8 later in the paper). In sum, the in vitro system lets the organelles go through a cycle of initial fragmentation and subsequent refusion, and it may allow the study of events that shift the balance from preferential fragmentation to preferential fusion.

In vitro fragmentation shares numerous properties with vacuole fragmentation in vivo

We tested whether the reconstituted reaction reflected properties of vacuole fragmentation in an intact cell. Complex cell biological reactions typically require an energy source, the presence of specific proteins, and a physiological temperature. Temperature dependence has been shown (Figure 2C). We next tested the ATP and cytosol dependence of the process. Whereas fragmentation proceeded efficiently in the presence of cytosolic proteins. it was reduced by >80% if cytosol was omitted from the reactions (Figure 3A). Omitting ATP or using EDTA to chelate the Mg^{2+} that is essential for hydrolysis of ATP reduced fragmentation by >90% (Figure 3B). Thus vacuole fragmentation in vitro is temperature-dependent and ATP-dependent and requires cytosolic factors.

Vacuole fragmentation in vivo depends on the dynamin-related GTPase Vps1p (Peters *et al.*, 2004) and on the production of phosphatidylinositol-3,5-bisphosphate (PI-3,5-P_2; Bonangelino *et al.*, 1997, 2002; Cooke *et al.*, 1998; Gary *et al.*, 1998; Jin *et al.*, 2008). We tested whether fragmentation in vitro reproduces these requirements.

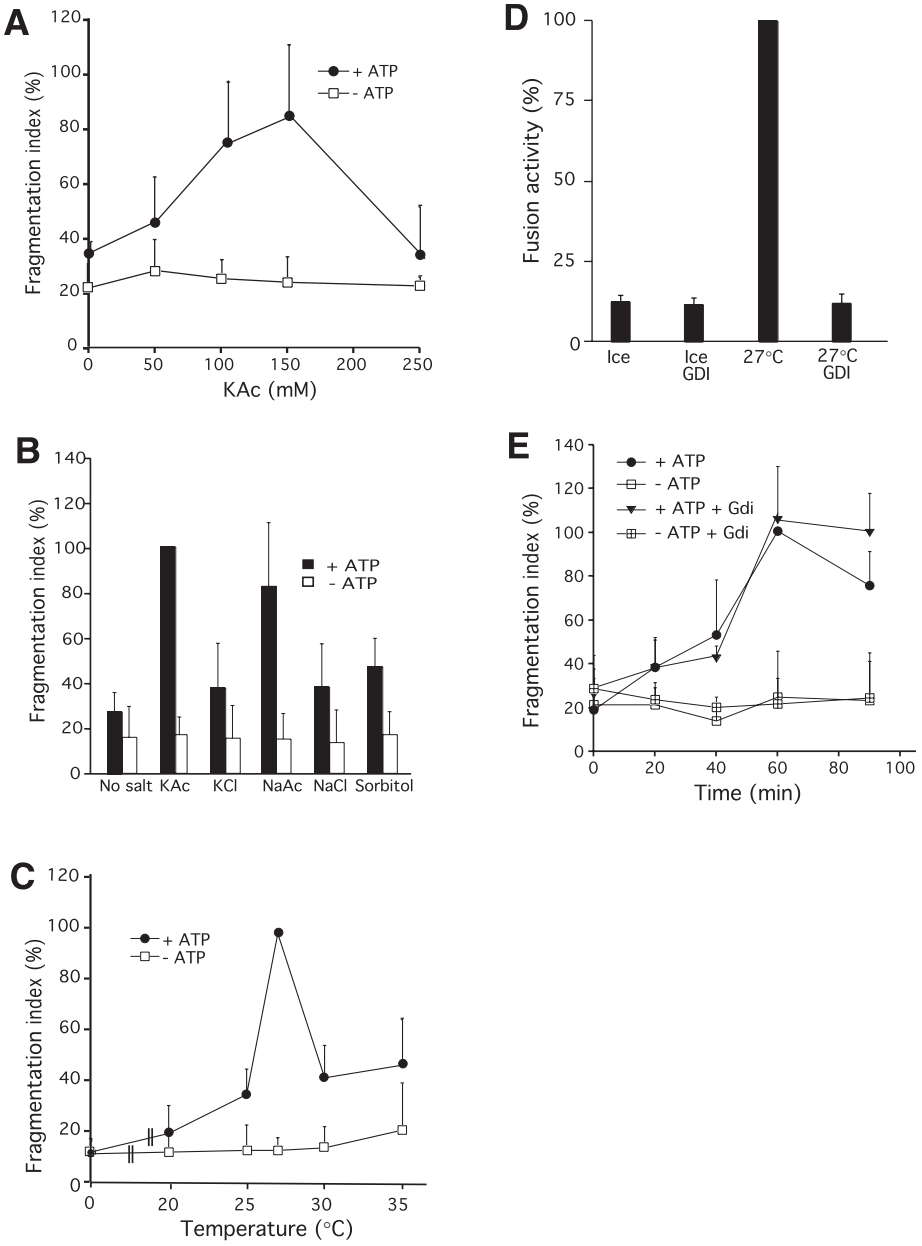

FIGURE 2: Parameters relevant to fragmentation in vitro. (A) Salt concentration. Fragmentation reactions were performed with 0, 50, 100, 150, and 250 mM of KAc. For each concentration, parallel reactions were set up with (positive control) and without ATP (negative control). $p < 0.03$ (–ATP vs. +ATP) at 100 and 150 mM KAc. (B) Ionic composition. Fragmentation reactions were performed with 100 mM of four different salts—KAc, KCl, NaCl, or NaAc—or with 300 mM sorbitol. Each solution was adjusted to a pH of 6.8. Values for KAc/+ATP were normalized to 100% before averaging. $p < 0.01$ for the differences between KAc and all other salts except NaAc. (C) Temperature. Fragmentation reactions were run for 60 min at 0, 20, 25, 27, 30, and 35°C with and without ATP. Values for 27°C/+ATP were normalized to 100% before averaging. $p < 0.01$ (–ATP vs. +ATP) for 25, 27, and 30°C. (D) Gdi1p suppresses fusion activity that can be measured under conditions of in vitro fragmentation. Reactions were run in the presence or absence of Gdi1p (10 μM) and an ATP regenerating system. After 70 min, fusion activity was determined. $p < 0.001$ for all differences relative to the 27°C/–GDI values. $n = 3$. (E) Time. Fragmentation reactions with and without ATP and Gdi1p (0.3 mg/ml) were run at 27°C for the indicated periods of time. Values for 60 min/+ATP were normalized to 100% before averaging. $p < 0.01$ (–ATP vs. +ATP) for all time points ≥20 min.

We purified vacuoles from a strain deleted for VPS1 (Δ*vps1*) or from a strain carrying a thermosensitive *vps1*^{ts} allele as the sole source of Vps1p (Ekena *et al.*, 1993). By use of a moderate salt shock, which induces rapid and synchronous vacuole fragmentation (Weisman, 2003), it was shown that Δ*vps1* cells have defects in vacuole fragmentation in vivo (Peters *et al.*, 2004). In the same assay, *vps1*^{ts} cells fragmented their vacuoles as in wild type at 25°C but not after brief incubation at 37°C, when the *vps1*^{ts} protein becomes nonfunctional (Figure 4A). In the in vitro assays vacuoles isolated from Δ*vps1* cells showed <15% of the fragmentation activity of wild-type vacuoles (Figure 4B). For testing the *vps1*^{ts} vacuoles in vitro the cells were grown at 25°C, the temperature at which *vps1*^{ts} remains functional (Ekena *et al.*, 1993). Before vacuole extraction, the cells were shifted to 37°C for 20 min. This treatment reduced the fragmentation activity of *vps1*^{ts} vacuoles by >80% (Figure 4C) compared with the wild-type control.

To inactivate Vps1p more acutely, we used affinity-purified antibodies to this protein. They allow us to rapidly interfere with Vps1p function on the surface of isolated wild-type vacuoles (Peters *et al.*, 2004). Incubation of the vacuoles with 0.5 μM anti-Vps1p suppressed fragmentation activity as efficiently as the omission of ATP (Figure 4D). Control antibodies, which bind the abundant vacuolar V-ATPase subunit Vph1p but do not inhibit its proton pump function (Bayer *et al.*, 2003), did not significantly inhibit fragmentation. These results suggest that the dynamin-like GTPase Vps1p is directly involved in vacuole fragmentation in vitro. The requirement for the PI-3,5-P_2 producing Fab1 complex was tested using a mutant deleted for the gene of its catalytic subunit Fab1p. Δfab1 cells do not fragment their vacuoles upon salt shock (Figure 4E; Bonangelino *et al.*, 2002). Vacuoles prepared from this mutant were also defective for fragmentation in vitro (Figure 4F). These observations confirm that in vitro fragmentation reproduces important aspects of the reaction in living cells.

In vitro vacuole fragmentation depends on the electrochemical potential and on GTP hydrolysis

The accessibility of the membranes in the in vitro system allows us to identify low–molecular weight inhibitors of fragmentation. We tested whether GTP hydrolysis is required to support vacuole fragmentation, by using GTPγS. This poorly hydrolysable analogue of GTP can arrest GTPases in the GTP-bound state and prevent their enzymatic cycling. GTPγS inhibited fragmentation in vitro by >90% (Figure 5A). The IC_{50} was 0.3 mM and complete inhibition occurred at 1 mM GTPγS (Figure 5B). GTPγS might inhibit fragmentation because it disassembles high–molecular weight forms of Vps1p

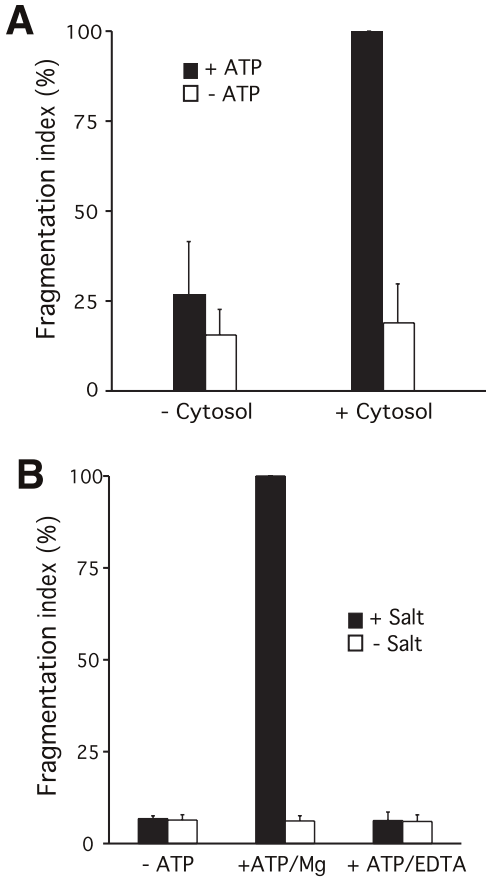

FIGURE 3: ATP and cytosol dependence of fragmentation in vitro. (A) Cytosolic factors. Fragmentation reactions were run in the presence or absence of cytosolic proteins (1 mg/ml). Values +cytosol/+ATP were normalized to 100% before averaging. $p < 001$ for the difference between +ATP values. (B) Energy source. In vitro fragmentation was performed in the presence or absence of ATP. Alternatively, hydrolysis of the ATP present in the sample was prevented by chelating Mg^{2+} with EDTA (7 mM). $p < 001$ for all differences relative to the +Mg/−ATP value.

and weakens their interaction with vacuoles (Peters *et al.*, 2004). A multimeric form of Vps1p is expected to support vacuole fragmentation, in analogy to the fission step in endocytosis, which depends on multimeric dynamin I (Muhlberg *et al.*, 1997; Sweitzer and Hinshaw, 1998). Using the in vitro system we could identify several other low–molecular weight inhibitors of vacuole fragmentation (Figure 5C). Among these were concanamycin A (2.5 μM), valinomycin (3 μM), carbonyl cyanide *p*-trifluoromethoxyphenyl hydrazone (FCCP; 10 μM), microcystin LR (2.5 μM), and rapamycin (7 μM). Valinomycin is a K^+ ionophore that interferes with the membrane potential. Concanamycin A inhibits vacuole acidification by blocking the proton pump activity of the vacuolar H^+-ATPase. FCCP is a protonophore that collapses the pH gradient across the vacuole membrane. We also tested the microtubule- and actin-directed drugs colchicine and latrunculin A, which had no significant influence. The effects of valinomycin, concanamycin, and FCCP suggest that fragmentation depends on the electrochemical potential across the membranes. Furthermore, the in vitro effects of these inhibitors are consistent with in vivo observations indicating that vacuoles in V-ATPase mutants cannot fragment and that concanamycin A suppresses vacuole fragmentation in wild-type cells (Baars *et al.*, 2007). This further supports the physiological authenticity of the reconstituted reaction.

Rapamycin-sensitive TOR complex 1 activity controls vacuole fragmentation

Vacuole fragmentation in vitro was also blocked by rapamycin (Figure 5C), a drug inhibiting TOR kinase activity in the TOR complex 1 (TORC1; Heitman *et al.*, 1991; Loewith *et al.*, 2002), and by microcystin LR, an inhibitor of protein phosphatases of types 1 and 2A (MacKintosh *et al.*, 1990). TOR is a regulator of cell growth, whose activity is down-regulated in starving cells, and PP2A activity mediates many TOR outputs (De Virgilio and Loewith, 2006). Rapamycin mimics this down-regulation and thus induces starvation responses, such as autophagy (Wullschleger *et al.*, 2006). Upon starvation or rapamycin treatment, the vacuoles in living yeast cells coalesce into a single big organelle, leading to a increase in vacuole size (Cardenas and Heitman, 1995; Catlett and Weisman, 2000; Crespo *et al.*, 2005; Dubouloz *et al.*, 2005).

Because vacuoles exist in an equilibrium of fusion and fragmentation in vivo (Baars *et al.*, 2007), we investigated whether these two processes are controlled by TOR. We used *tor1-1/tor2-1* double mutants, which express rapamycin-resistant alleles of the two TOR genes in yeast, TOR1 and TOR2. Many TOR-dependent processes—at least those essential for growth—are less sensitive to the drug in this strain (Wullschleger *et al.*, 2006). We isolated vacuoles from *tor1-1/tor2-1* double mutants and wild-type strains and compared their fragmentation activities in the presence of rapamycin (Figure 6A). Rapamycin inhibited the fragmentation of wild-type vacuoles to the background levels observed in the absence of ATP, whereas vacuoles from the rapamycin-resistant *tor1-1/tor2-1* cells retained their activity. Note that all fragmentation reactions were performed with cytosol from wild-type TOR1/TOR2 cells. That vacuoles isolated from *tor1-1/tor2-1* cells retain their rapamycin resistance indicates that the relevant pool of TOR is associated with the vacuoles and does not readily diffuse into the cytosol. This is consistent with the fact that in living cells one of the two TOR complexes is bound to vacuoles (Sturgill *et al.*, 2008).

We tested the authenticity of this in vitro result in the in vivo situation, using the induction of vacuole fragmentation by hypertonic shock (Bonangelino *et al.*, 2002). Vacuole membranes in living yeast cells were stained with the fluorescent vital dye FM4-64 (Vida and Emr, 1995). Upon addition of 0.4 M NaCl to the medium, wild-type cells rapidly (<10 min) fragmented their large vacuoles into multiple small vesicles (Figure 6, B and C). Cells preincubated with rapamycin for 40 min did not show this reaction. In contrast, *tor1-1/tor2-1* cells fragmented their vacuoles equally well in the presence or absence of rapamycin. Because TOR functions via two large protein complexes, TORC1 and TORC2, we investigated which complex is responsible for vacuole fragmentation. The fact that TORC1 is localized on vacuoles (Sturgill *et al.*, 2008) and that only TORC1 but not TORC2 is sensitive to rapamycin (Loewith *et al.*, 2002) points to TORC1. We tested this further by deleting the gene for the nonessential TORC1 subunit *Tco89p* (Reinke *et al.*, 2004) and assaying vacuole structure of the cells before and after NaCl treatment (Figure 7A). Already in normal medium, Δ*tco89* cells showed fewer and slightly larger vacuoles than the wild type. Upon addition of NaCl, the Δ*tco89* cells did not show the pronounced increase in vacuole number that is observable in wild-type cells. Vacuoles prepared from Δ*tco89* cells showed a corresponding deficiency for ATP-dependent fragmentation in vitro (Figure 7B). Collectively these data suggest that fragmentation of the vacuolar compartment is positively regulated by TORC1 in vivo and in vitro and that TORC1 activity is necessary for executing the fragmentation signal provided by hypertonic shock.

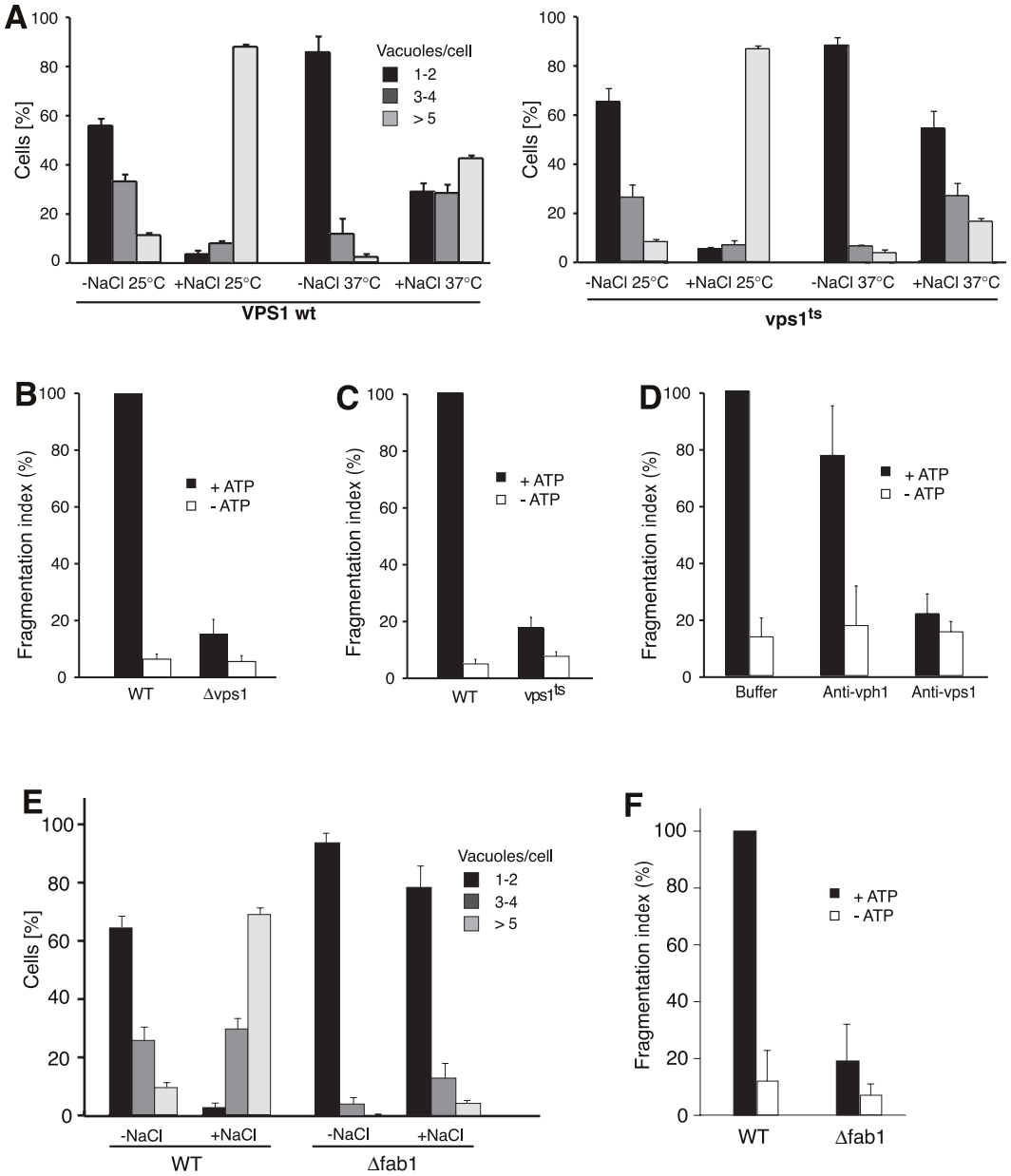

FIGURE 4: Fragmentation of vacuoles from *vps1* and *fab1* mutants. (A) Fragmentation in vivo. *vps1*^{ts} mutants or isogenic wild-type cells were grown to logarithmic phase at 25°C and stained with FM4-64. Then the cells were split and either shifted to 37°C for 20 min or left at 25°C. The medium was supplemented with 0.4 M NaCl. After further 10 min at 25 or 37°C, cells were centrifuged and immediately analyzed by fluorescence microscopy. The cells (>100 per condition and experiment) were evaluated and classified according to the number of vacuoles visible per cell. (B) Vacuoles were prepared from BJ3505 wild-type or isogenic Δ*vps1*-knockout strains. Fission activity of the organelles in vitro was assayed in presence or absence of ATP. Values for WT/+ATP were normalized to 100% before averaging. $p < 0.001$ for all differences relative to the WT+ATP value. n = 3. (C) Temperature-sensitive Vps1p. BJ3505 Δvps1 was complemented with centromeric plasmids expressing wild-type *VPS1* or a thermosensitive allele, *vps1*^{ts} (Ekena *et al.*, 1993). The cells were grown overnight at permissive temperature (25°C) and subjected to a 20-min temperature shock (37°C) during the spheroplasting step of vacuole preparation. Vacuoles isolated from these cells were compared in in vitro fragmentation assays in the presence and absence of ATP. Values for WT/+ATP were normalized to 100% before averaging. $p < 0.001$ for all differences relative to the WT/+ATP value. n = 3. (D) Inhibition of fragmentation by antibodies to Vps1p. Vacuoles were isolated from wild-type BJ3505 cells. The organelles were analyzed in in vitro fragmentation reactions containing affinity-purified antibodies to Vps1p (0.5 μM) or, as a negative control, the same concentration of antibodies to the vacuolar membrane protein Vph1p. $p < 0.01$ for all differences relative to the buffer/+ATP value. (E) Δ*fab1* mutants and corresponding wild-type cells, both in Δ*pep4* background (Mayer *et al.*, 2000), were grown to logarithmic phase (OD_{600} = 1) and stained with FM4-64. The culture medium was supplemented with 0.4 M NaCl. After 10 min at 25°C, cells were centrifuged and immediately analyzed by fluorescence microscopy. The cells (>100 per condition and experiment) were evaluated and classified according to the number of vacuoles visible per cell. n = 3. (F) Vacuoles were prepared from Δ*fab1* mutants and corresponding wild-type cells. The in vitro fission activity of the organelles was assayed as in B.

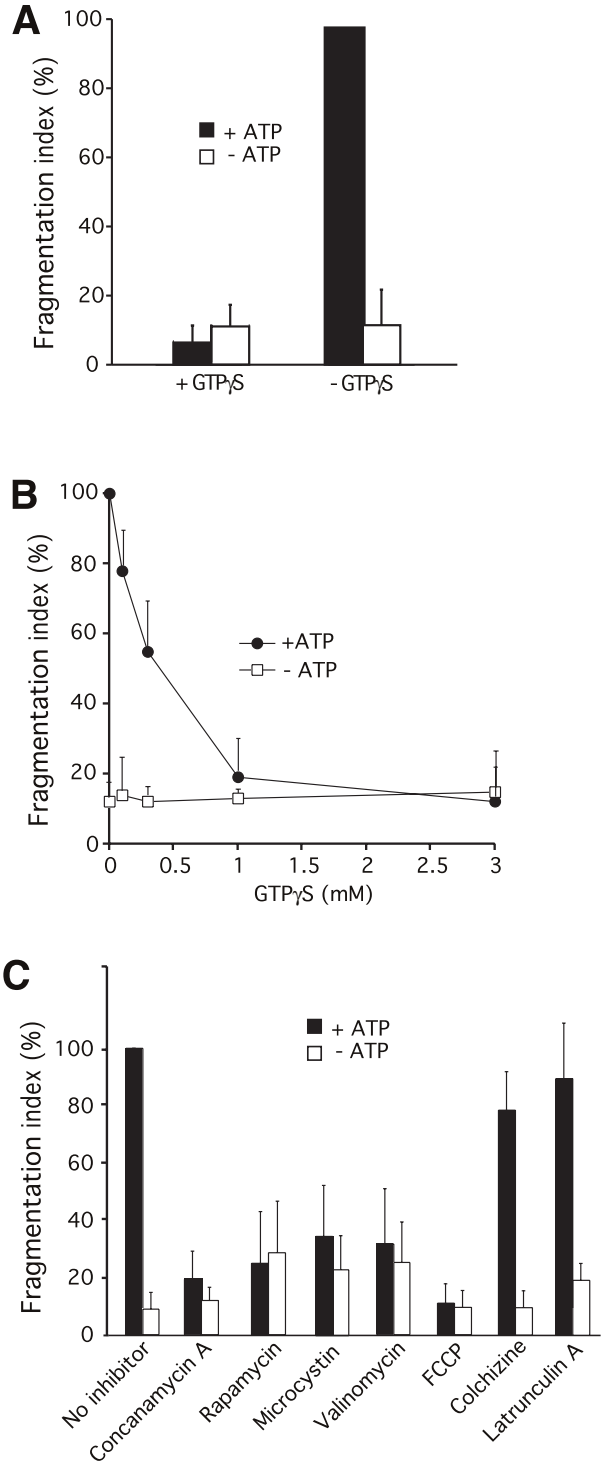

FIGURE 5: Sensitivity of fragmentation to low–molecular weight inhibitors. (A) Poorly hydrolysable GTP analogue. Vacuoles from BJ3505 wild-type cells were subjected to fragmentation reactions with and without ATP in the presence or absence of 1 mM GTPγS. $p < 0.001$ for all differences relative to the –GTPγS/+ATP value. (B) As in A, but the concentration of GTPγS was varied as indicated. $p < 0.001$ (–ATP vs. +ATP) for concentrations of <1 mM. (C) Inhibitors of TOR or of the electrochemical potential. Fragmentation reactions were run as in A, but with concanamycin A (2.5 μM), rapamycin (7 μM), valinomycin (3 μM), FCCP (10 μM), microcystin LR (25 μM), latrunculin A (10 μM), colchicine (1 mM), or without inhibitor (DMSO solvent only). $p < 0.01$ for all differences relative to the –inhibitor/+ATP value. Values –inhibitor/+ATP were normalized to 100% before averaging for A–C.

Vacuole fragmentation depends on the PP2A-like phosphatase Sit4p

Few direct target proteins for TOR have been identified in yeast. Among these are the TORC1 targets Sch9p and Sfp1p, as well as Ypk1p/2p, Slm1p, and Slm2p, which act in TORC2 signaling (Audhya *et al.*, 2004; Kamada *et al.*, 2005; Urban *et al.*, 2007; Lempiainen *et al.*, 2009). Conditional ATP analogue–sensitive alleles of SCH9 did not interfere with vacuole fragmentation, and the constitutively active allele $SCH9^{2D3E}$ (Urban *et al.*, 2007) did not render vacuole fragmentation rapamycin resistant. Equivalent mutants for YPK1 and deletion mutants for SLM1, SLM2, and SFP1 had no effects on vacuole fragmentation either (data not shown). TORC1 signaling often implicates the PP2A-like phosphatase Sit4p and the PP2A Pph21p/Pph22p. Deletion of the PP2A-like SIT4 inhibited fragmentation (Figure 8A). Sit4p binds to Tap42p, a cofactor that can be phosphorylated by TORC1 and that controls Sit4p and Pph21/Pph22p activities in many essential TOR-dependent processes (Di Como and Arndt, 1996; Gorner *et al.*, 1999; Jacinto *et al.*, 2001; Duvel and Broach, 2004). We tested the role of Tap42p and of its major downstream targets for vacuole fragmentation. Strains expressing the temperature-sensitive alleles *tap42-106*, *tap42-109* (Duvel *et al.*, 2003), or *tap42-11* (Di Como and Arndt, 1996) as the sole source of Tap42p fragmented their vacuoles as efficiently as those carrying a wild-type allele, even at restrictive temperature (Figure 8, B and C). This suggests that vacuole fragmentation might be regulated by a signaling branch that depends on Sit4p and TORC1 but is insensitive to the conditional *tap42* alleles used here.

Vacuole fusion is largely rapamycin insensitive

Both fragmentation and fusion activities determine vacuole structure in vivo (Baars *et al.*, 2007). An apparent inhibition of vacuole fragmentation by rapamycin could thus have three reasons: A genuine inhibition of fragmentation activity by rapamycin, a stimulation of fusion activity, or a combination of both effects. Because our microscopic observations (see prior discussion) suggested that fusion was possible and prevailed upon prolonged incubation of the vacuoles in our fragmentation assay, we tested a potential influence of TORC1 on fusion using an in vitro assay system for vacuole fusion. This assay reproduces numerous physiological aspects of vacuole fusion. It is based on the proteolytic conversion of pro–alkaline phosphatase in one fusion partner by the appropriate maturation enzymes provided by the other fusion partner (Haas *et al.*, 1994). The assay was used to score fusion activity after 60 min of incubation under the conditions that support in vitro fragmentation of vacuoles ("fragmentation conditions") or under conditions that had been optimized to study vacuole fusion only ("fusion conditions"; Reese *et al.*, 2005). Even under conditions optimized to reconstitute in vitro vacuole fragmentation, the vacuoles showed significant fusion activities, reaching more than half of the signal obtainable under conditions optimized for vacuole fusion. Thus both fusion and fragmentation can occur during the in vitro fragmentation assay. However, in contrast to fragmentation, which is sensitive to rapamycin, fusion activity was only weakly affected (Figure 9). Of importance, it did not show the increase that would have been required to explain a potential interference of the fusion machinery with the apparent vacuole fragmentation activity. This suggests that rapamycin-sensitive TOR activity regulates vacuole fragmentation rather than fusion.

DISCUSSION

In response to nutrient restriction the vacuoles of yeast cells coalesce into a single organelle of strongly increased volume,

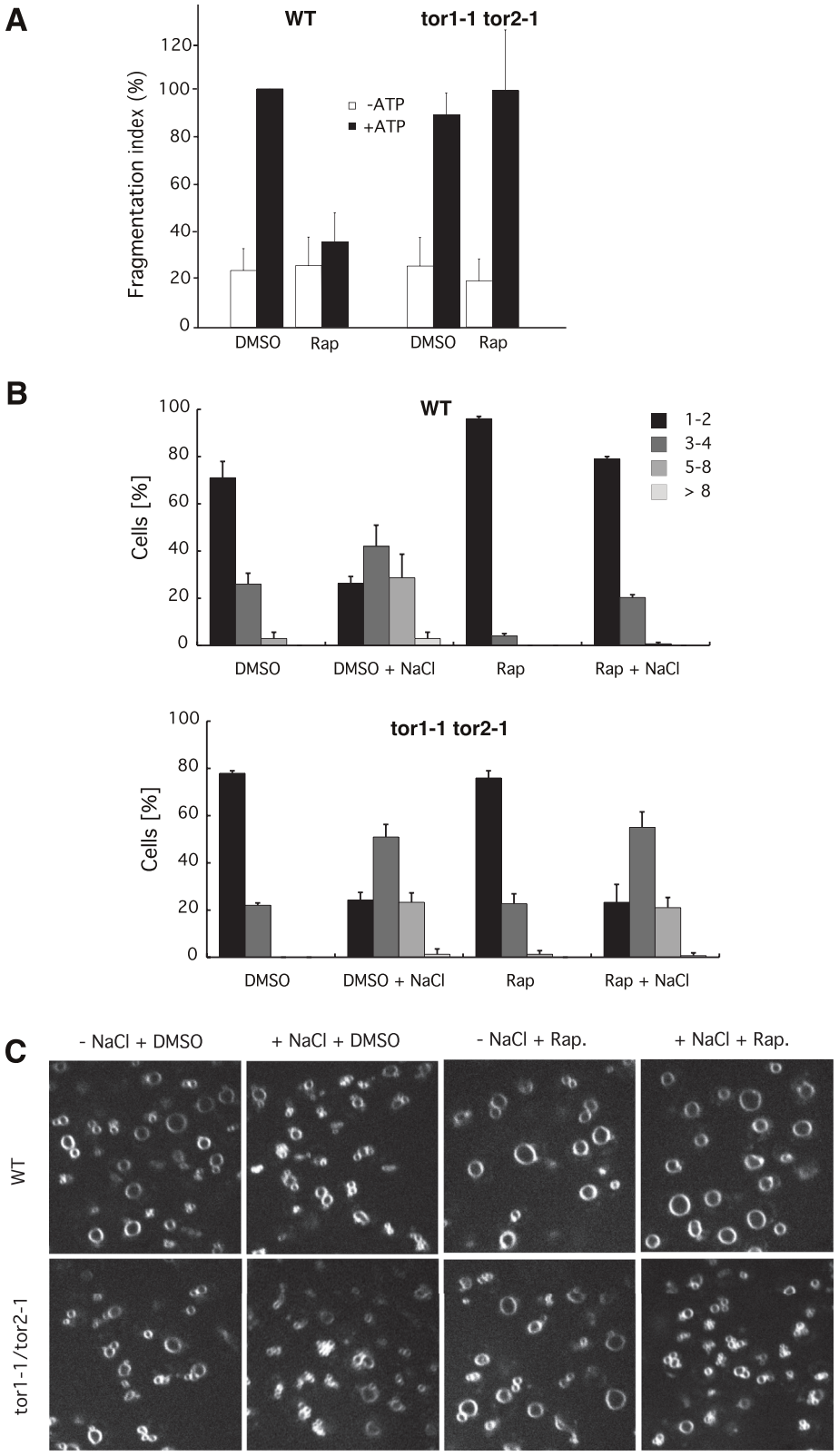

FIGURE 6: TOR and rapamycin dependence of vacuole fragmentation. (A) Vacuoles were isolated from *tor1-1/tor2-1* double mutants or from isogenic wild-type cells. Fragmentation reactions were run in vitro in the presence or absence of rapamycin (7 μM) and ATP. $p < 0.01$ for the difference of the +ATP/+rapamycin values. (B) Fragmentation in vivo. *tor1-1/tor2-1* double mutants or isogenic wild-type cells were grown to logarithmic phase and stained with FM4-64. Rapamycin (2 μM from a 100× stock in DMSO) or DMSO was added to the cultures. Cells were incubated for 40 min at 25°C with shaking. The culture medium was supplemented with 0.4 M NaCl. After 10 min at 25°C, cells were centrifuged and immediately analyzed by fluorescence microscopy. The cells (>100 per condition and experiment) were evaluated and classified according to the number of vacuoles visible per cell. n = 3. (C) Representative confocal images of the vacuoles in groups of cells analyzed in B.

probably reflecting the need for increased hydrolytic capacity for autophagy (Baba *et al.*, 1994). TORC1 is a key factor in nutrient signaling (Wullschleger *et al.*, 2006). Our study demonstrates that TORC1 stimulates vacuole fragmentation, one of the two elementary processes controlling rapid adjustments of vacuole size and copy number. Because vacuole structure is defined by an equilibrium of fusion and fragmentation, starvation-induced down-regulation of TORC1 can suffice to induce vacuole coalescence by decreasing the ratio of the rates of fragmentation and fusion (Figure 10). Vacuole coalescence could result from a decrease in fragmentation activity, an increase in fusion activity, or both. Our data indicate that TORC1 activity can be limiting for vacuole fragmentation but not for vacuole fusion. This suggests that coalescence of the vacuolar compartment under starvation conditions is determined by down-regulation of fragmentation in the face of a constitutive opposing fusion activity, resulting in the formation of a single large organelle.

Few organelle fragmentation reactions have been reconstituted in vitro, such as mitotic fragmentation of the Golgi and the nuclear envelope or the separation of endosomal/lysosomal hybrid organelles (Pfaller and Newport, 1995; Pryor *et al.*, 2000; Shorter and Warren, 2002; Colanzi *et al.*, 2003). They are all based on higher eukaryotic cells. In yeast cells, which are genetically more tractable, organelle fragmentation has so far only been studied in vivo (Hoppins *et al.*, 2007; Nagotu *et al.*, 2010). Yeast vacuoles offer advantages for studying organelle fragmentation. They have a diameter of ≤5 μm and a simple structure, that is, their limiting membrane can be clearly visualized by fluorescence microscopy. Furthermore, hypertonic shock induces rapid and quantitative vacuole fragmentation in vivo (Bonangelino *et al.*, 2002), which facilitates mutant screening. Using this criterion, we screened the 4881 nonessential yeast genes for defects in vacuole fragmentation (Michaillat and Mayer, unpublished results). Dissection of this complex cell-biological reaction is facilitated by combining this in vivo approach with an in vitro system that reconstitutes

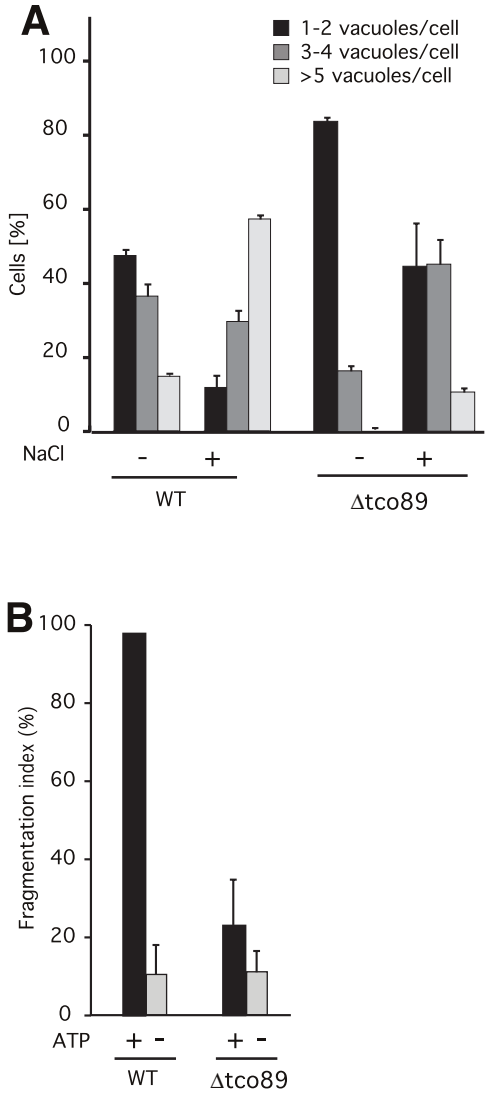

FIGURE 7: Fragmentation activity of Δ*tco89* mutants. (A) Δ*tco89* mutants and corresponding wild-type cells were grown to logarithmic phase (OD_{600} = 1) and stained with FM4-64. The culture medium was supplemented with 0.4 M NaCl. After 10 min at 25°C, cells were centrifuged and immediately analyzed by fluorescence microscopy. The cells (>100 per condition and experiment) were evaluated and classified according to the number of vacuoles visible per cell. n = 3. (B) Vacuoles were prepared from Δ*tco89* mutants and corresponding wild-type cells. The in vitro fission activity of the organelles was assayed as in Figure 4B.

vacuole fragmentation in a physiologically relevant form. The fragmentation reaction reconstituted here shares with the in vivo process its sensitivities to low–molecular weight inhibitors and numerous requirements, such as dependence on Vps1p, V-ATPase pump activity, the electrochemical potential, and TORC1 and Fab1. It did not show discrepancies from any known requirements for vacuole fragmentation. This indicates that the in vitro system reiterates important aspects of the physiological process. The system is read out by confocal microscopy, followed by counting the numbers of large and small vacuoles, which limits throughput. Despite these inconveniences, the cell-free system is a major advance, allowing analyses of the fragmentation process that are more difficult or even impossible in vivo. This includes the addition or withdrawal of individual proteins, the use of antibodies to selectively inactivate

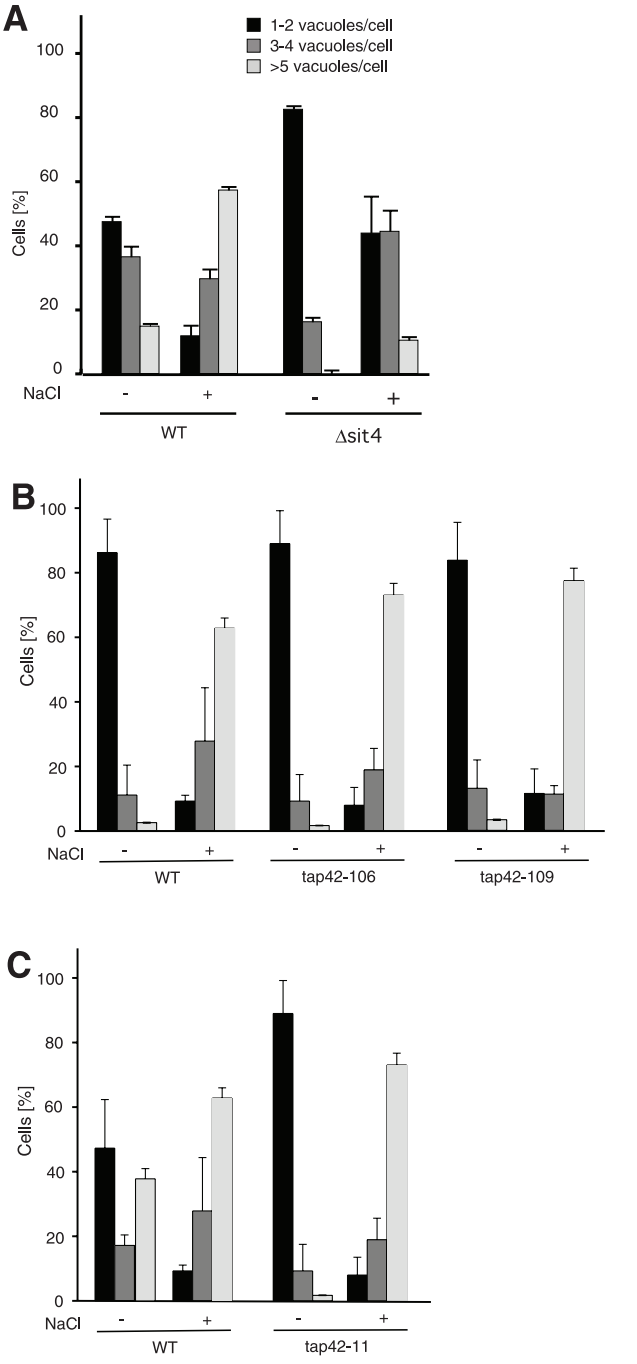

FIGURE 8: Vacuole fragmentation in mutants related to TORC1 signaling. (A) Vacuole fragmentation in Δ*sit4* mutants in vivo. Deletion mutants for SIT4 and isogenic wild-type (BY4742) cells were grown to logarithmic phase (OD_{600} = 1) and stained with FM4-64. The culture medium was supplemented with 0.4 M NaCl. After 10 min at 25°C, cells were centrifuged and immediately analyzed by fluorescence microscopy. The cells (>100 per condition and experiment) were evaluated and classified according to the number of vacuoles visible per cell. n = 3. (B, C) Vacuole fragmentation in *tap42* mutants. Cells carrying the temperature-sensitive alleles *tap42-106* or *tap42-109* (Duvel *et al.*, 2003), *tap42-11* (Di Como and Arndt, 1996), or the corresponding wild-type TAP42 allele were grown to logarithmic phase (OD_{600} = 1) and stained with FM4-64 at 25°C in YPD. After a shift to 37°C (40 min for *tap42-11*, 60 min for *tap42-106* and *tap42-109*), the medium was supplemented with 0.4 M NaCl. After 10 min of further incubation at 37°C, cells were analyzed for vacuole fragmentation as in A. n = 3.

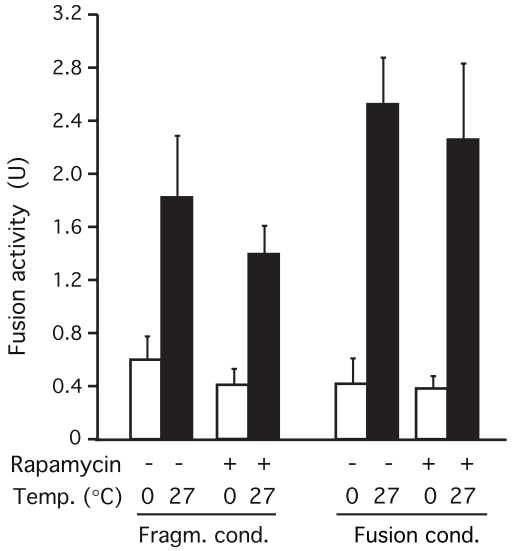

FIGURE 9: Effect of rapamycin on vacuole fusion. Vacuoles were isolated from BJ3505 and DKY6281 strains and used in in vitro reactions optimized for fragmentation or for fusion. The vacuoles were mixed and incubated in the presence or absence of rapamycin. After 90 min at 27°C or on ice, fusion activity was assayed in both sets of samples via the activity of the alkaline phosphatase reporter enzyme. p = 0.35 (+rapamycin vs. –rapamycin for fragmentation conditions).

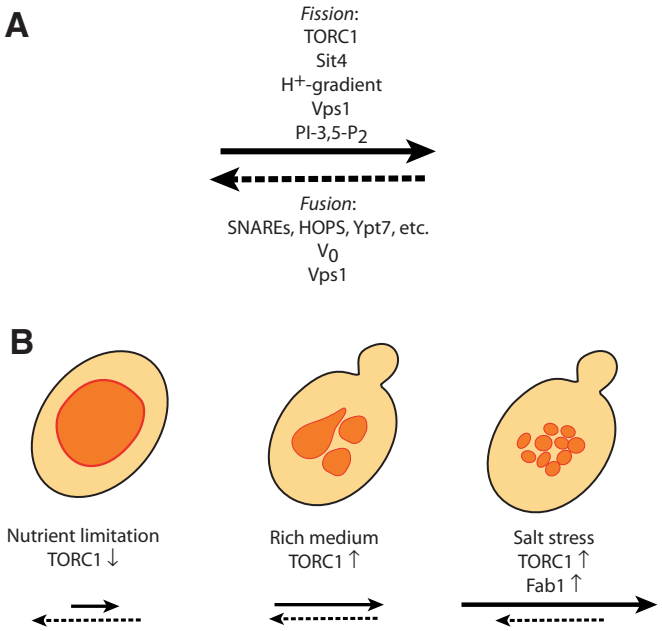

FIGURE 10: (A) Components involved in vacuole fusion and fragmentation and (B) their influence on the fusion–fission equilibrium under different conditions. The scheme shows only components relevant to this study and not all components involved in fusion and fission.

individual proteins on the organelle surface, the use of cell-impermeable inhibitors, and the dissection of the reaction into intermediates. Therefore the in vitro system provides additional tools that are not available in microscopic in vivo analyses.

Vacuole fragmentation and fusion are in an equilibrium that determines vacuole structure (Weisman, 2003; Baars *et al.*, 2007). Both reactions also occurred in our in vitro reactions. Whether net fragmentation or fusion of the organelle becomes apparent then depends on the ratio of the rates of these two reactions. This necessitates some precautions since a stimulation of fusion activity could shift the equilibrium and hence be misinterpreted as an inhibition of fragmentation. We addressed this problem in two ways. First, we used only inhibitors and mutants that are known not to stimulate fusion: GTPγS (Haas *et al.*, 1994; Reese and Mayer, 2005), concanamycin A (Bayer *et al.*, 2003; Muller *et al.*, 2003), rapamycin, valinomycin, and FCCP (Mayer *et al.*, 1996; Peters *et al.*, 2001), antibodies to the V-ATPase (Bayer *et al.*, 2003), withdrawal of ATP or prevention of its hydrolysis by EDTA (Conradt *et al.*, 1994; Mayer *et al.*, 1996), Δ*vps1* and *vps1*^{ts} (Peters *et al.*, 2004), withdrawal of cytosol (Conradt *et al.*, 1992), and GDI (Haas *et al.*, 1995). We verified and confirmed the lack of stimulation of fusion by these reagents under our assay conditions (data not shown). Second, fragmentation activity strongly predominates during the initial 60 min of the reaction. This predominance is sufficiently pronounced so that even addition of GDI, which reduces fusion activity by >90% (Figure 2E), does not significantly accelerate the kinetics of apparent fragmentation. Therefore, it appears that the changes in vacuole size and number are mainly defined via fragmentation activity during the first 60 min of incubation. The reappearance of large vacuoles, which occurs upon prolonged incubations, suggests that fusion can dominate the equilibrium at later time points. This is an interesting and potentially useful phenomenon. Whether it reproduces a physiological switch that lets the organelles go through an obligatory cycle of fragmentation and subsequent coalescence in the test tube must be carefully tested in future studies. Such a regulated switch might shift the fusion/fragmentation equilibrium to control organelle size and number, for example, in response to osmo- or nutrient-sensing signaling networks. The TOR requirement identified here could be part of such a mechanism.

Why do vacuoles fragment? Vacuoles fragment and fuse as part of the mechanism for their transmission to daughter cells (Weisman, 2003). They fulfill important functions in hydrolysis, osmoregulation, and storage of amino acids and ions (Klionsky *et al.*, 1990) and modify their shape, number, and size in response to environmental changes. During logarithmic growth, cells of most yeast strains contain two to five vacuoles of intermediate size. Upon hypertonic shock, vacuoles fragment. They rapidly (<1 min) lose water and volume, but the membrane surface seems to remain constant. Transfer into hypotonic media promotes the opposite reaction—vacuole coalescence. Vacuoles may respond in this way because fragmentation and coalescence allow them to rapidly readjust their surface-to-volume ratio. This ratio determines membrane tension on the organelle, which in turn might influence central vacuolar functions, such as the activity of vacuolar transporters and ion channels. Vacuoles also coalesce into a single big organelle upon nutrient limitation and entry into stationary phase. Because starvation strongly induces the expression of vacuolar hydrolases (Knop *et al.*, 1993), the resulting increase in hydrolytic capacity probably necessitates an expansion of the vacuolar volume in order to facilitate the degradation of large amounts of cytoplasmic material, which autophagy transfers into vacuoles under these conditions (Baba *et al.*, 1994). Control over fragmentation and fusion of vacuoles could thus adjust vacuole size and number to physiological changes. It might, in addition, adjust vacuole volume and number to growth of the other cell constituents, that is, to integrate vacuole growth with the growth of the rest of the cell. Testing this hypothesis and separating these two aspects will require the identification of the relevant TORC1 targets on vacuoles.

The precise analysis of signaling events downstream of TORC1 was not the purpose of our study, but we nevertheless obtained information on a few candidate pathways. In contrast to Cdc28p, for which many targets are known, few direct target proteins for TOR have been identified. Our experiments did not reveal a role for any of them in vacuolar fragmentation. In addition, knockouts of key genes involved in TORC1-controlled pathways, such as the stress response pathway (MSN2, MSN4) and the nitrogen discrimination pathway (GLN3, URE2, GAT1), did not show effects on vacuole fragmentation. Many known outputs of TORC1 activity are regulated via PP2A- and PP2A-like protein phosphatases. Astonishingly, we identified a strong fragmentation defect for Δ*sit4* mutants but not for *tap42-106*, *tap42-109*, or *tap42-11* mutants, which affect TORC1 control over SIT4 in other PP2A-regulated pathways (Di Como and Arndt, 1996; Jacinto *et al.*, 2001; Duvel *et al.*, 2003; De Virgilio and Loewith, 2006). This TAP42-dependent branch of TORC1 signaling has mainly been characterized using processes essential for survival. Vacuole fragmentation, which is nonessential under rich growth conditions (Weisman, 2003), provides an example for a TORC1 output that may be controlled via PP2A in a way that is independent of TAP42, or at least insensitive to the three well-characterized conditional alleles we used. It might implicate other associations of PP2As, such as those with Cdc55p, Rts1p, and Tpd3p, or, for Sit4p, with the SAP proteins (Jablonowski *et al.*, 2009).

Development of cells depends on the coordination of proliferation and cell growth. These aspects are controlled by two central kinases—the cyclin-dependent kinase Cdc28p, which governs proliferation via the cell cycle, and TOR kinase, which regulates growth (Wullschleger *et al.*, 2006). Whereas there are examples of organelle fragmentation being linked to the cell cycle and to control by Cdc28p, for example for the Golgi (Shorter and Warren, 2002; Colanzi *et al.*, 2003) or for the nuclear envelope (Newport and Forbes, 1987), TOR has remained largely unexplored in these respects. A recent observation links mTOR activity to the behavior of mammalian lysosomes. Upon starvation and induction of autophagy, lysosomes fuse with many newly formed autophagosomes, thereby forming enlarged hybrid organelles—autolysosomes. During exit from the starved state, which reactivates mTOR, autolysosomes shed tubular and vesicular structures, which are assumed to be substrates for re-forming lysosomes (Yu *et al.*, 2010; Rong *et al.*, 2011). This shedding of large vesicular and tubular structures is a membrane fission reaction and in this sense equivalent to the vacuolar fragmentation that we studied. Apparent fragmentation of autolysosomes could result from an inhibition of fusion or from a stimulation of fission activity by mTOR. In analogy to our observations, we propose that mTOR activity selectively stimulates the (auto-) lysosomal fission machinery in order to trigger regeneration of lysosomes.

MATERIALS AND METHODS

Strains

See Table 1.

Reagents

Reagents included BODIPY FL-DHPE (Molecular Probes, Invitrogen, Carlsbad, CA), FM4-64 (Molecular Probes), concanamycin A (Alexis Biochemicals, San Diego, CA), rapamycin (Alexis), valinomycin (Sigma-Aldrich, St. Louis, MO), FCCP (Sigma-Aldrich), GTPγS (Roche, Indianapolis, IN), and microcystin LR (Alexis). Polyclonal antibodies to Vps1p and Vph1p were produced by injecting the soluble proteins subcutaneously into rabbit (Vps1p) or goat (Vph1p). Antibodies were affinity purified from the serum. Gdi1p was recombinantly expressed and purified from *Escherichia coli* (Mayer *et al.*, 1996).

Cytosol preparation

Ten l of *S. cerevisiae* strain K91-1A were grown to early logarithmic phase in yeast extract/peptone/dextrose (YPD; 150 rpm, 30°C). Cells were harvested (5 min, 4°C, 4200 × *g*) and resuspended in one pellet volume of chilled cytosol buffer (200 mM sorbitol, 40 mM 1,4-piperazinediethanesulfonic acid [PIPES]/KOH, pH 6.8, 0.5 mM $MgCl_2$, 1 mM dithiothreitol [DTT], 1 mM phenylmethylsufonylfluoride, and 1× protease inhibitor cocktail: 0.1 mM Pefablock SC [Roche], 0.2 µM leupeptin, 0.1 mM *o*-phenanthrolin, and 0.75 µM pepstatin A). Cells were pooled, centrifuged (5 min, 4°C, 4200 × *g*), and resuspended in cytosol buffer as a thick slurry. A thin stream of the slurry was poured into liquid nitrogen, yielding nuggets of frozen cells. They were cracked for 5–10 min in a Waring blender filled with liquid nitrogen. The homogenized powder was thawed and centrifuged (20 min, 4°C, 4000 × *g*). The supernatant was centrifuged again (Beckman Ti45 rotor, 30 min, 4°C, 120,000 × g). Lipid was aspirated from the top, and the supernatant was centrifuged as before. The cytosol was filtered (0.2 µm), adjusted to 30 mg/ml protein concentration with cytosol buffer, frozen in 100-µl aliquots in liquid nitrogen, and stored at –80°C.

Lyticase preparation

β-1,3-Glucanase from *Oerskovia xanthineolytica* was expressed in *E. coli* strain RSB 805. The protein was purified from the periplasmic space. A 10-l amount of RSB 805 was grown in Luria Bertani (LB) medium (5 g/l yeast extract, 10 g/l tryptone, 5 g/l NaCl) with 100 µg/ml ampicillin to OD_{600} = 0.6. Isopropyl-β-D-thiogalactoside 0.4 mM was added, and, after another 5 h at 30°C, cells were harvested (10 min, room temperature, 4200 × *g*), washed with 50 ml of washing buffer (25 mM Tris/Cl, pH 7.4), and centrifuged as before. Pellets were resuspended in 200 ml of washing buffer, supplemented with 2 mM EDTA and an equal volume of 40% (wt/vol) sucrose in washing buffer, and gently shaken at room temperature for 20 min. Cells were harvested (10 min, room temperature, 4200 × *g*), and the supernatant was completely removed. Flasks were chilled on ice. The cells from 1 l of culture were resuspended in 20 ml of ice-cold 0.5 mM $MgSO_4$, gently shaken (4°C, 20 min), and centrifuged (10 min, 4°C, 4200 × *g*). Protein concentration of the supernatant varied around 1 mg/ml.

Vacuole isolation

For vacuole preparation, cells were precultured in YPD medium overnight (30°C, 150 rpm). Logarithmic cultures were inoculated (30°C, 14–16 h, 150 rpm) in baffled 2-l Erlenmeyer flasks with 1 l of YPD. At OD_{600} = 1.6–1.8, cells were centrifuged (3 min, 4000 × *g*, 4°C, JLA-10.500 rotor), resuspended in 50 ml of 0.1 M Tris/HCl (pH 8.9) with 10 mM DTT, incubated (7 min, 30°C), centrifuged (2 min, 4000 × *g*, 4°C), resuspended in 15 ml of SB (50 mM KP_i, pH 7.5, 600 mM sorbitol in YPD with 0.2% glucose and 8 mg/ml lyticase), and transferred into 30-ml Corex tubes. Cells were incubated (25 min, 30°C), reisolated (2 min, 4000 × *g*, 4°C, JA20 rotor), and gently resuspended in 2.5 ml of 15% Ficoll 400 in PS buffer (10 mM PIPES/KOH, pH 6.8, 200 mM sorbitol). DEAE-dextrane (300 µl) was added from a fresh stock (0.4 mg/ml) in 15% Ficoll in PS. The cells were incubated (2 min, 30°C), chilled again, transferred to a SW41 tube, and overlaid with 3 ml of 8% Ficoll, 3 ml of 4% Ficoll, and 1.5 ml of 0% Ficoll (all in PS). After centrifugation (75 min, 150,000 × *g*, 2°C), vacuoles were harvested from the 0–4% interphase. Water purity is a critical issue, which can influence the obtainable absolute fragmentation activities. In the course of these studies we noted that purification of the water used for the media over a charcoal cartridge enhances the absolute activities of the vacuoles for some strain backgrounds, such as TB50.

Strain	Genotype	Source or reference	Strain	Genotype	Source or reference
BJ3505	Mat a *pep4::HIS3 prb1-D1.6R lys2-208 trp1-D101 ura3-52 gal2 can*	Pieren *et al.* (2010)	TB50a	Mat a; *leu2-3, ura3-52; trp1; rme1;his3D GAL+ HMLa*	R. Loewith; Heitman *et al.* (1991)
DKY6281	Mat a *leu2-3, -112 ura3-52 his3-Δ200 trp1-Δ901 lys2-801 suc2-Δ9 pho8::TRP1*	Pieren *et al.* (2010)	RL206-4d	TB50a *TOR1-1 TOR2-1*	R. Loewith
Δvps1	BJ3505 Δ*vps1*	Peters *et al.* (2004)	tap42-11	TB50a sch9::kanMX tap42::HphMX4 + pRS414::SCH9wt + pRS415::tap42-11ts	R. Loewith
vps1wt	BJ3505 Δ*vps1* + *p416GPD vps1wt*	Ekena *et al.* (1993)	tap42 wt	TB50a sch9::kanMX tap42::HphMX4 + pRS414::SCH9wt + pRS415::tap42wt	R. Loewith
vps1ts	BJ3505 Δ*vps1* + *p416GPD vps1ts*	Ekena *et al.* (1993)	sch9 2D3E	TB50a sch9::kanMX tap42::HphMX4 + pRS414::sch9D3E + pRS415::TAP42wt	R. Loewith
BY4741	MATα his3Δ1 met15Δ0 ura3Δ0	Brachmann *et al.* (1998)	sch9 as	TB50a sch9::kanMX + pRS414::SCH9as (Sch9T492G)	R. Loewith
BY4741/2	MATα his3Δ1 leu2Δ0 lys2Δ0 ura3Δ0	Brachmann *et al.* (1998)	ypk1 as	TB50a ypk1::kanMX ypk2::HIS3MX + pRS461::YPK1as	R. Loewith
Δtco89	BY4741/2 Δ*tco89*	R. Loewith	ypk1 wt	TB50a ypk1::kanMX ypk2::HIS3MX + pRS461::YPK1wt	R. Loewith
Δure2	BY4741 Δ*ure2*	This study	Δtor1	BY4741 Δ*tor1*	EUROSCARF
Δgln3	BY4741 Δ*gln3*	EUROSCARF	Δsfp1	BY4741 Δ*sfp1*	EUROSCARF
Δgat1	BY4741 Δ*gat1*	EUROSCARF	Δmsn2	BY4741 Δmsn2	EUROSCARF
Δsit4	BY4741 Δ*sit4*	This study	Δmsn4	BY4741 Δmsn4	EUROSCARF
W303-1A	MAT a ade2-1 can1-100 his3-11 15leu2-3 112trp1-1 ura3-1 GAL	Duvel *et al.* (2003)	Δrtg1	BY4741 Δrtg1	EUROSCARF
Y3033	W303-1A tap42::HIS3 + pRS414-TAP42 wt	Duvel *et al.* (2003)	Δrtg3	BY4741 Δrtg3	EUROSCARF
Y3034	W303-1A tap42::HIS3 + pRS414-tap42-106 ts	Duvel *et al.* (2003)	Δmpk1	BY4741 Δmpk1	EUROSCARF
Y3035	W303-1A tap42::HIS3 + pRS414-tap42-109 ts	Duvel *et al.* (2003)	Δnpr1	BY4741 Δnpr1	EUROSCARF
			Δmks1	BY4741 Δmks1	EUROSCARF

EUROSCARF, European *Saccharomyces cerevisiae* Archive for Functional Analysis, Institute for Molecular Biosciences, Johann Wolfgang Goethe-University Frankfurt, Frankfurt, Germany. R. Loewith, University of Geneva, Geneva, Switzerland .
Plasmids introduced into strains are denoted by a +.

TABLE 1: Strains used in this work.

Vacuole fragmentation in vitro

Reactions contained 3 μg of vacuoles in 30 μl of reaction buffer (20 mM PIPES/KOH, pH 6.8, 200 mM sorbitol, 5 mM $MgCl_2$, 0.75 mM ATP, 1 mg/ml K91-1A cytosol extract, 0.2× protease inhibitor cocktail [final concentration 40 μM Pefablock SC, 2.1 μM leupeptin, 80 μM *o*-phenanthrolin, 1.5 μM pepstatin A], 30 mM creatine phosphate, 52.5 U/ml creatine kinase, and 100 mM or 150 mM KAc). The optimal KAc concentration differed between experiments due to batch differences in the culture media. The experiments were hence performed with two concentrations of KAc—100 and 150 mM—and the one resulting in the higher control activities was chosen to evaluate the experiment. To suppress the competing fusion activity, 0.3 mg/ml GDI (Reese *et al.*, 2005) can be added (this was used, e.g., for experiments involving *tor1-1/tor2-1* mutants). The ATP regenerating system, containing $MgCl_2$, ATP, creatine phosphate, and creatine kinase, was added from a frozen stock. Creatine kinase was stored at –20°C in 10 mM PIPES/KOH, pH 6.8, and 50% glycerol. Negative controls without ATP contained creatine phosphate and PS buffer but no ATP and creatine kinase. Fragmentation reactions were incubated for 60 min at 27°C. Then vacuoles in the 30-μl reaction were stained with 2 μl of BODIPY FL-DHPE (10 μg/ml in 70% ethanol). A 3-μl amount was withdrawn and mixed with 6 μl of 0.2% LMP-agarose held at 37°C. A 1-μl amount of this suspension was transferred to cavity slides and analyzed by fluorescence confocal microscopy (Zeiss [Thornwood, NY] LSM 510; excitation 488 nm, 100×/1.4 numerical aperture PlanNeofluoar, electronic zoom 2, pinhole size 1.00 Airy unit). Laser intensity was 32.5, detector gain was 880, amplifier offset was –0.287, and amplifier gain was 1.

As an alternative, reactions could also be performed in poly-L-lysine–coated chambers. Coverglass chambers (Lab-Tek 155411; Nalge Nunc International, Rochester, NY) were washed once with ethanol 70% and twice with sterile water. After drying, a solution of poly-L-lysine (0.1% wt/vol) in water was added in the chamber and incubated at room temperature for 10 min. Then the solution was removed and the chamber was closed and stored at room temperature

overnight. Coated chambers were used for fragmentation assays the next day. An 800-µl amount of vacuoles with a concentration of 0.3–0.5 mg/ml in PS buffer was stained with 10 µM rhodamine 123 for 3 min at 27°C. Then 500 µl of 15% Ficoll 400 in PS was added and mixed gently. The suspension was transferred into siliconized 2-ml Eppendorf tubes and overlaid with 300 µl of 4% Ficoll in PS and 400 µl of PS. The tubes were centrifuged (10 min, 8900 × *g*, 2°C), and the vacuoles were recovered from the 0–4% interphase. Vacuoles were incubated 30 min at room temperature in the coated chamber. Then the chambers were washed twice with PS, making sure to always keep some liquid in the chamber to avoid drying of the vesicles. Finally, the buffer was supplemented to a complete reaction mixture, and the chambers were incubated at 27°C for 1 h and directly analyzed by confocal fluorescence microscopy.

Quantification of the reaction in vitro

Pictures were taken close to the coverslip, where vacuoles sediment, or at the bottom of the chamber. Vacuoles were counted and grouped into classes according to their diameter d: small, $d \leq 0.6$ µm; medium, $0.6\ \mu m < d < 1.5\ \mu m$; large, $d \geq 1.5$ µm. Vacuolar fragments in clusters were often too small and numerous to permit direct counting. Therefore their number was approximated via the area they occupied in the pictures (using the software ImageJ [National Institutes of Health, Bethesda, MD]). The number of small vacuolar fragments in the section was calculated by dividing this area by the area of an average small vacuole that has a diameter of 0.4 µm. The numbers of large, medium, and small vacuoles (N_l, N_m, and N_s, respectively) were used to calculate the ratio $R = N_s/(N_s + N_m + N_l)$. To simplify representation and comparisons of fragmentation activity, we defined a fragmentation index FI: $FI = R_{pos}/R \times 100$ (%), where R_{pos} is the ratio for the positive control and R the ratio for the sample to be evaluated. Pictures of seven random fields per sample, containing the membrane equivalent to 10–50 vacuoles, were taken. The minimal number of vacuole equivalents analyzed was 200 per condition and experiment. FI of the positive controls (+ATP) ranged between 100 and 400 for all experiments evaluated.

Electron microscopy

Vacuoles were subjected to 10× fragmentation reactions. At the end of the reaction period the samples were supplemented with 2% glutaraldehyde, incubated for 30 min on ice, and supplemented with 50 µM glycine. After centrifugation (15 min, 100,000 × *g*, 4°C) the supernatant was withdrawn. The pellet was resuspended in 500 µl of buffer F (0.1 M Na-phosphate, pH 7.3, 200 mM sorbitol), centrifuged as before. This wash was repeated, and the final pellet was resuspended in a small volume of 1% agarose in buffer F. After solidification, we added 2% OsO_4 in buffer F, incubated at room temperature (1 h), washed again with buffer F, and dehydrated in a series of 50, 70, 90, and 100% ethanol. Finally, the pellet was incubated with an ethanol/epon (1:1) mixture (30 min) and then with pure epon overnight at ambient temperature. After polymerization at 60°C (3 d), the samples were cut and analyzed by electron microscopy.

Vacuole fusion assay

Fusion reactions were performed either under fragmentation conditions as described earlier or under conditions promoting only fusion as described in Peters *et al*. (2004): 3 µg of each type of purified vacuole (DKY6281 and BJ3505) was incubated in a total volume of 30 µl of reaction buffer (20 mM PIPES/KOH, pH6.8, 200 mM sorbitol, 120 mM KCl, 0.5 mM $MnCl_2$, 0.5 mM $MgCl_2$, 0.5 mM ATP, 20 µM Pefablock SC, 1 µM leupeptin, 40 µM *o*-phenanthrolin, 0.75 µM pepstatin A, 20 mM creatine phosphate, and 35 U/ml creatine kinase). After 60 min at 27°C, alkaline phosphatase activity was determined by conversion of *p*-nitrophenol phosphate, which can be measured as change in OD_{400}.

In vivo vacuole fragmentation

Yeast was precultured in YPD or selective medium (25°C). Overnight cultures were grown (14–16 h, 25°C, 150 rpm) in logarithmic phase ($OD_{600} < 1$). To visualize vacuolar membranes, in vivo cells were stained with FM4-64 (Vida and Emr, 1995). cultures were adjusted to $OD_{600} = 0.4$, and 10 µM FM4–64 was added from a 100 mM stock in dimethyl sulfoxide (DMSO). Cells were incubated for 1 h at 25°C, harvested (1 min, 3000 × *g*), washed twice in fresh medium, resuspended in YPD at $OD_{600} = 0.4$, and shaken for 1–2 h at 25°C. Fragmentation was induced by adding 0.4 M NaCl. After 10 min at 25°C, cells were centrifuged (15 s, 8000 × *g*), resuspended in 0.05 volume of the supernatant, and immediately analyzed by spinning disk confocal fluorescence microscopy (QLC100; Visitron, Puchheim, Germany) at minimal intensity of excitation light (488 nm). To quantify vacuole morphology, photos of at least 10 random fields were taken. The number of vacuolar vesicles in 100 cells per experiment and condition was determined, and cells were grouped into three categories: 1–2, 3–4, or >5 vacuoles per cell. Data from at least three independent experiments were averaged and the standard deviations calculated.

Statistics

Data from three to five independent experiments were averaged. Error bars represent the SD. Statistical significance was tested using Student's *t* test.

ACKNOWLEDGMENTS

We thank Robbie Loewith, Claudio de Virgilio, Jim Broach, and Tom Stevens for strains; Monique Reinhardt, Véronique Comte, and Andrea Schmidt for assistance; and the Cellular Imaging Facility for support with microscopy. This work was supported by the Swiss National Science Foundation, the European Research Council, and the Human Frontier and Science Program.

REFERENCES

Acharya U, Mallabiabarrena A, Acharya JK, Malhotra V (1998). Signaling via mitogen-activated protein kinase kinase (MEK1) is required for Golgi fragmentation during mitosis. Cell 92, 183–192.

Antonny B (2006). Membrane deformation by protein coats. Curr Opin Cell Biol 18, 386–394.

Audhya A, Loewith R, Parsons AB, Gao L, Tabuchi M, Zhou H, Boone C, Hall MN, Emr SD (2004). Genome-wide lethality screen identifies new PI4,5P2 effectors that regulate the actin cytoskeleton. EMBO J 23, 3747–3757.

Baars TL, Petri S, Peters C, Mayer A (2007). Role of the V-ATPase in regulation of the vacuolar fission-fusion equilibrium. Mol Biol Cell 18, 3873–3882.

Baba M, Takeshige K, Baba N, Ohsumi Y (1994). Ultrastructural analysis of the autophagic process in yeast: detection of autophagosomes and their characterization. J Cell Biol 124, 903–913.

Bayer MJ, Reese C, Buhler S, Peters C, Mayer A (2003). Vacuole membrane fusion: V0 functions after trans-SNARE pairing and is coupled to the Ca2+-releasing channel. J Cell Biol 162, 211–222.

Bleazard W, McCaffery JM, King EJ, Bale S, Mozdy A, Tieu Q, Nunnari J, Shaw JM (1999). The dynamin-related GTPase Dnm1 regulates mitochondrial fission in yeast. Nat Cell Biol 1, 298–304.

Bonangelino CJ, Catlett NL, Weisman LS (1997). Vac7p, a novel vacuolar protein, is required for normal vacuole inheritance and morphology. Mol Cell Biol 17, 6847–6858.

Bonangelino CJ, Nau JJ, Duex JE, Brinkman M, Wurmser AE, Gary JD, Emr SD, Weisman LS (2002). Osmotic stress-induced increase of phosphatidylinositol 3,5-bisphosphate requires Vac14p, an activator of the lipid kinase Fab1p. J Cell Biol 156, 1015–1028.

Brachmann CB, Davies A, Cost GJ, Caputo E, Li J, Hieter P, Boeke JD (1998). Designer deletion strains derived from *Saccharomyces cerevisiae* S288C: a useful set of strains and plasmids for PCR-mediated gene disruption and other applications. Yeast 14, 115–132.

Cardenas ME, Heitman J (1995). FKBP12-rapamycin target TOR2 is a vacuolar protein with an associated phosphatidylinositol-4 kinase activity. EMBO J 14, 5892–5907.

Catlett NL, Weisman LS (2000). Divide and multiply: organelle partitioning in yeast. Curr Opin Cell Biol 12, 509–516.

Chan DC (2006). Mitochondrial fusion and fission in mammals. Annu Rev Cell Dev Biol 22, 79–99.

Colanzi A, Suetterlin C, Malhotra V (2003). Cell-cycle-specific Golgi fragmentation: how and why? Curr Opin Cell Biol 15, 462–467.

Conner SD, Schmid SL (2003). Regulated portals of entry into the cell. Nature 422, 37–44.

Conradt B, Haas A, Wickner W (1994). Determination of four biochemically distinct, sequential stages during vacuole inheritance in vitro. J Cell Biol 126, 99–110.

Conradt B, Shaw J, Vida T, Emr S, Wickner W (1992). In vitro reactions of vacuole inheritance in *Saccharomyces cerevisiae*. J Cell Biol 119, 1469–1479.

Cooke FT, Dove SK, McEwen RK, Painter G, Holmes AB, Hall MN, Michell RH, Parker PJ (1998). The stress-activated phosphatidylinositol 3-phosphate 5-kinase Fab1p is essential for vacuole function in *S. cerevisiae*. Curr Biol 8, 1219–1222.

Corda D, Hidalgo Carcedo C, Bonazzi M, Luini A, Spano S (2002). Molecular aspects of membrane fission in the secretory pathway. Cell Mol Life Sci 59, 1819–1832.

Crespo JL, Diaz-Troya S, Florencio FJ (2005). Inhibition of target of rapamycin signaling by rapamycin in the unicellular green alga *Chlamydomonas reinhardtii*. Plant Physiol 139, 1736–1749.

De Virgilio C, Loewith R (2006). Cell growth control: little eukaryotes make big contributions. Oncogene 25, 6392–6415.

Di Como CJ, Arndt KT (1996). Nutrients, via the Tor proteins, stimulate the association of Tap42 with type 2A phosphatases. Genes Dev 10, 1904–1916.

Dove SK, McEwen RK, Mayes A, Hughes DC, Beggs JD, Michell RH (2002). Vac14 controls PtdIns(3,5)P(2) synthesis and Fab1-dependent protein trafficking to the multivesicular body. Curr Biol 12, 885–893.

Dove SK *et al*. (2004). Svp1p defines a family of phosphatidylinositol 3,5-bisphosphate effectors. EMBO J 23, 1922–1933.

Dubouloz F, Deloche O, Wanke V, Cameroni E, De Virgilio C (2005). The TOR and EGO protein complexes orchestrate microautophagy in yeast. Mol Cell 19, 15–26.

Duex JE, Nau JJ, Kauffman EJ, Weisman LS (2006a). Phosphoinositide 5-phosphatase Fig 4p is required for both acute rise and subsequent fall in stress-induced phosphatidylinositol 3,5-bisphosphate levels. Eukaryot Cell 5, 723–731.

Duex JE, Tang F, Weisman LS (2006b). The Vac14p-Fig4p complex acts independently of Vac7p and couples PI3,5P2 synthesis and turnover. J Cell Biol 172, 693–704.

Duvel K, Broach JR (2004). The role of phosphatases in TOR signaling in yeast. Curr Top Microbiol Immunol 279, 19–38.

Duvel K, Santhanam A, Garrett S, Schneper L, Broach JR (2003). Multiple roles of Tap42 in mediating rapamycin-induced transcriptional changes in yeast. Mol Cell 11, 1467–1478.

Efe JA, Botelho RJ, Emr SD (2005). The Fab1 phosphatidylinositol kinase pathway in the regulation of vacuole morphology. Curr Opin Cell Biol 17, 402–408.

Efe JA, Botelho RJ, Emr SD (2007). Atg18 regulates organelle morphology and Fab1 kinase activity independent of its membrane recruitment by phosphatidylinositol 3,5-bisphosphate. Mol Biol Cell 18, 4232–4244.

Ekena K, Vater CA, Raymond CK, Stevens TH (1993). The VPS1 protein is a dynamin-like GTPase required for sorting proteins to the yeast vacuole. Ciba Found Symp 176, 198–211discussion, 211–214.

Gao H, Kadirjan-Kalbach D, Froehlich JE, Osteryoung KW (2003). ARC5, a cytosolic dynamin-like protein from plants, is part of the chloroplast division machinery. Proc Natl Acad Sci USA 100, 4328–4333.

Gary JD, Sato TK, Stefan CJ, Bonangelino CJ, Weisman LS, Emr SD (2002). Regulation of Fab1 phosphatidylinositol 3-phosphate 5-kinase pathway by Vac7 protein and Fig4, a polyphosphoinositide phosphatase family member. Mol Biol Cell 13, 1238–1251.

Gary JD, Wurmser AE, Bonangelino CJ, Weisman LS, Emr SD (1998). Fab1p is essential for PtdIns(3)P 5-kinase activity and the maintenance of vacuolar size and membrane homeostasis. J Cell Biol 143, 65–79.

Gorner W, Schuller C, Ruis H (1999). Being at the right place at the right time: the role of nuclear transport in dynamic transcriptional regulation in yeast. Biol Chem 380, 147–150.

Haas A, Conradt B, Wickner W (1994). G-protein ligands inhibit in vitro reactions of vacuole inheritance. J Cell Biol 126, 87–97.

Haas A, Scheglmann D, Lazar T, Gallwitz D, Wickner W (1995). The GTPase Ypt7p of *Saccharomyces cerevisiae* is required on both partner vacuoles for the homotypic fusion step of vacuole inheritance. EMBO J 14, 5258–5270.

Heitman J, Movva NR, Hall MN (1991). Targets for cell cycle arrest by the immunosuppressant rapamycin in yeast. Science 253, 905–909.

Higa MM, Ullman KS, Prunuske AJ (2006). Studying nuclear disassembly in vitro using *Xenopus* egg extract. Methods 39, 284–290.

Hoepfner D, van den Berg M, Philippsen P, Tabak HF, Hettema EH (2001). A role for Vps1p, actin, and the Myo2p motor in peroxisome abundance and inheritance in *Saccharomyces cerevisiae*. J Cell Biol 155, 979–990.

Hoppins S, Lackner L, Nunnari J (2007). The machines that divide and fuse mitochondria. Annu Rev Biochem 76, 751–780.

Jablonowski D, Taubert JE, Bar C, Stark MJ, Schaffrath R (2009). Distinct subsets of Sit4 holophosphatases are required for inhibition of *Saccharomyces cerevisiae* growth by rapamycin and zymocin. Eukaryot Cell 8, 1637–1647.

Jacinto E, Guo B, Arndt KT, Schmelzle T, Hall MN (2001). TIP41 interacts with TAP42 and negatively regulates the TOR signaling pathway. Mol Cell 8, 1017–1026.

Jin N *et al*. (2008). VAC14 nucleates a protein complex essential for the acute interconversion of PI3P and PI(3,5)P(2) in yeast and mouse. EMBO J 27, 3221–3234.

Kamada Y, Fujioka Y, Suzuki NN, Inagaki F, Wullschleger S, Loewith R, Hall MN, Ohsumi Y (2005). Tor2 directly phosphorylates the AGC kinase Ypk2 to regulate actin polarization. Mol Cell Biol 25, 7239–7248.

Kano F, Takenaka K, Yamamoto A, Nagayama K, Nishida E, Murata M (2000). MEK and Cdc2 kinase are sequentially required for Golgi disassembly in MDCK cells by the mitotic *Xenopus* extracts. J Cell Biol 149, 357–368.

Klionsky DJ, Herman PK, Emr SD (1990). The fungal vacuole: composition, function, and biogenesis. Microbiol Rev 54, 266–292.

Knop M, Schiffer HH, Rupp S, Wolf DH (1993). Vacuolar/lysosomal proteolysis: proteases, substrates, mechanisms. Curr Opin Cell Biol 5, 990–996.

Kuravi K, Nagotu S, Krikken AM, Sjollema K, Deckers M, Erdmann R, Veenhuis M, van der Klei IJ (2006). Dynamin-related proteins Vps1p and Dnm1p control peroxisome abundance in *Saccharomyces cerevisiae*. J Cell Sci 119, 3994–4001.

LaGrassa TJ, Ungermann C (2005). The vacuolar kinase Yck3 maintains organelle fragmentation by regulating the HOPS tethering complex. J Cell Biol 168, 401–414.

Lempiainen H, Uotila A, Urban J, Dohnal I, Ammerer G, Loewith R, Shore D (2009). Sfp1 interaction with TORC1 and Mrs6 reveals feedback regulation on TOR signaling. Mol Cell 33, 704–716.

Li X, Gould SJ (2003). The dynamin-like GTPase DLP1 is essential for peroxisome division and is recruited to peroxisomes in part by PEX11. J Biol Chem 278, 17012–17020.

Loewith R, Jacinto E, Wullschleger S, Lorberg A, Crespo JL, Bonenfant D, Oppliger W, Jenoe P, Hall MN (2002). Two TOR complexes, only one of which is rapamycin sensitive, have distinct roles in cell growth control. Mol Cell 10, 457–468.

Luzio JP, Poupon V, Lindsay MR, Mullock BM, Piper RC, Pryor PR (2003). Membrane dynamics and the biogenesis of lysosomes. Mol Membr Biol 20, 141–154.

MacKintosh C, Beattie KA, Klumpp S, Cohen P, Codd GA (1990). Cyanobacterial microcystin-LR is a potent and specific inhibitor of protein phosphatases 1 and 2A from both mammals and higher plants. FEBS Lett 264, 187–192.

Mancias JD, Goldberg J (2005). Exiting the endoplasmic reticulum. Traffic 6, 278–285.

Mayer A, Scheglmann D, Dove S, Glatz A, Wickner W, Haas A (2000). Phosphatidylinositol 4,5-bisphosphate regulates two steps of homotypic vacuole fusion. Mol Biol Cell 11, 807–817.

Mayer A, Wickner W, Haas A (1996). Sec18p (NSF)-driven release of Sec17p (alpha-SNAP) can precede docking and fusion of yeast vacuoles. Cell 85, 83–94.

McMahon HT, Gallop JL (2005). Membrane curvature and mechanisms of dynamic cell membrane remodelling. Nature 438, 590–596.

Misteli T, Warren G (1994). COP-coated vesicles are involved in the mitotic fragmentation of Golgi stacks in a cell-free system. J Cell Biol 125, 269–282.

Muhlberg AB, Warnock DE, Schmid SL (1997). Domain structure and intramolecular regulation of dynamin GTPase. EMBO J 16, 6676–6683.
Muller O, Neumann H, Bayer MJ, Mayer A (2003). Role of the Vtc proteins in V-ATPase stability and membrane trafficking. J Cell Sci 116, 1107–1115.
Nagotu S, Veenhuis M, van der Klei IJ (2010). Divide et impera: the dictum of peroxisomes. Traffic 11, 175–184.
Newport JW, Forbes DJ (1987). The nucleus: structure, function, and dynamics. Annu Rev Biochem 56, 535–565.
Okamoto K, Shaw JM (2005). Mitochondrial morphology and dynamics in yeast and multicellular eukaryotes. Annu Rev Genet 39, 503–536.
Osteryoung KW, McAndrew RS (2001). The plastid division machine. Annu Rev Plant Physiol Plant Mol Biol 52, 315–333.
Ostrowicz CW, Meiringer CT, Ungermann C (2008). Yeast vacuole fusion: a model system for eukaryotic endomembrane dynamics. Autophagy 4, 5–19.
Peplowska K, Markgraf DF, Ostrowicz CW, Bange G, Ungermann C (2007). The CORVET tethering complex interacts with the yeast Rab5 homolog Vps21 and is involved in endo-lysosomal biogenesis. Dev Cell 12, 739–750.
Peters C, Baars TL, Buhler S, Mayer A (2004). Mutual control of membrane fission and fusion proteins. Cell 119, 667–678.
Peters C, Bayer MJ, Buhler S, Andersen JS, Mann M, Mayer A (2001). Trans-complex formation by proteolipid channels in the terminal phase of membrane fusion. Nature 409, 581–588.
Pfaller R, Newport JW (1995). Assembly/disassembly of the nuclear envelope membraneCharacterization of the membrane-chromatin interaction using partially purified regulatory enzymes. J Biol Chem 270, 19066–19072.
Pieren M, Schmidt A, Mayer A (2010). The SM protein Vps33 and the t-SNARE H(abc) domain promote fusion pore opening. Nat Struct Mol Biol 17, 710–717.
Prunuske AJ, Ullman KS (2006). The nuclear envelope: form and reformation. Curr Opin Cell Biol 18, 108–116.
Pryor PR, Mullock BM, Bright NA, Gray SR, Luzio JP (2000). The role of intraorganellar Ca(2+) in late endosome-lysosome heterotypic fusion and in the reformation of lysosomes from hybrid organelles. J Cell Biol 149, 1053–1062.
Rabouille C, Jokitalo E (2003). Golgi apparatus partitioning during cell division. Mol Membr Biol 20, 117–127.
Rabouille C, Misteli T, Watson R, Warren G (1995). Reassembly of Golgi stacks from mitotic Golgi fragments in a cell-free system. J Cell Biol 129, 605–618.
Reese C, Heise F, Mayer A (2005). Trans-SNARE pairing can precede a hemifusion intermediate in intracellular membrane fusion. Nature 436, 410–414.
Reese C, Mayer A (2005). Transition from hemifusion to pore opening is rate limiting for vacuole membrane fusion. J Cell Biol 171, 981–990.
Reinke A, Anderson S, McCaffery JM, Yates J 3rd, Aronova S, Chu S, Fairclough S, Iverson C, Wedaman KP, Powers T (2004). TOR complex 1 includes a novel component, Tco89p (YPL180w), and cooperates with Ssd1p to maintain cellular integrity in *Saccharomyces cerevisiae*. J Biol Chem 279, 14752–14762.
Rong Y *et al*. (2011). Spinster is required for autophagic lysosome reformation and mTOR reactivation following starvation. Proc Natl Acad Sci USA 108, 7826–7831.
Schrader M, Fahimi HD (2006). Growth and division of peroxisomes. Int Rev Cytol 255, 237–290.
Shaw JM, Nunnari J (2002). Mitochondrial dynamics and division in budding yeast. Trends Cell Biol 12, 178–184.
Shorter J, Warren G (1999). A role for the vesicle tethering protein, p115, in the post-mitotic stacking of reassembling Golgi cisternae in a cell-free system. J Cell Biol 146, 57–70.
Shorter J, Warren G (2002). Golgi architecture and inheritance. Annu Rev Cell Dev Biol 18, 379–420.
Storrie B, Desjardins M (1996). The biogenesis of lysosomes: is it a kiss and run, continuous fusion and fission process? Bioessays 18, 895–903.
Sturgill TW, Cohen A, Diefenbacher M, Trautwein M, Martin DE, Hall MN (2008). TOR1 and TOR2 have distinct locations in live cells. Eukaryot Cell 7, 1819–1830.
Sweitzer SM, Hinshaw JE (1998). Dynamin undergoes a GTP-dependent conformational change causing vesiculation. Cell 93, 1021–1029.
Urban J *et al*. (2007). Sch9 is a major target of TORC1 *in Saccharomyces cerevisiae*. Mol Cell 26, 663–674.
van der Goot FG, Gruenberg J (2006). Intra-endosomal membrane traffic. Trends Cell Biol 16, 514–521.
Vida TA, Emr SD (1995). A new vital stain for visualizing vacuolar membrane dynamics and endocytosis in yeast. J Cell Biol 128, 779–792.
Weisman LS (2003). Yeast vacuole inheritance and dynamics. Annu Rev Genet 37, 435–460.
Weisman LS, Bacallao R, Wickner W (1987). Multiple methods of visualizing the yeast vacuole permit evaluation of its morphology and inheritance during the cell cycle. J Cell Biol 105, 1539–1547.
Wickner W (2010). Membrane fusion: five lipids, four SNAREs, three chaperones, two nucleotides, and a Rab, all dancing in a ring on yeast vacuoles. Annu Rev Cell Dev Biol 26, 115–136.
Wullschleger S, Loewith R, Hall MN (2006). TOR signaling in growth and metabolism. Cell 124, 471–484.
Yan M, Rayapuram N, Subramani S (2005). The control of peroxisome number and size during division and proliferation. Curr Opin Cell Biol 17, 376–383.
Yoon Y, McNiven MA (2001). Mitochondrial division: new partners in membrane pinching. Curr Biol 11, R67–R70.
Yu L *et al*. (2010). Termination of autophagy and reformation of lysosomes regulated by mTOR. Nature 465, 942–946.